ANALYSIS OF DIFFERENT TI5553 ALLOY CUTTING STRATEGIES FOR THE IMPROVEMENT OF TOOL LIFE

ANALYSIS OF DIFFERENT TI5553 ALLOY CUTTING STRATEGIES FOR THE IMPROVEMENT OF TOOL LIFE

By TARCISIO KOCK FILHO, B. ENG.

A Thesis Submitted to the School of Graduate Studies in Partial Fulfillment of the Requirements for the Degree Master of Applied Sciences

McMaster University MASTER OF APPLIED SCIENCE (2021) Hamilton, Ontario

(Mechanical Engineering)

TITLE: ANALYSIS OF DIFFERENT TI5553 ALLOY CUTTING STRATEGIES FOR THE IMPROVEMENT OF TOOL LIFE.

AUTHOR: Tarcisio Kock Filho B. Eng., Mechanical Engineering

SUPERVISOR: Dr. Stephen C. Veldhuis

NUMBER OF PAGES: xv, 89.

ABSTRACT

Titanium alloys support a wide range of practical applications due to their excellent mechanical properties. These include high strength-to-weight ratio, high mechanical strength at elevated temperatures and remarkable oxidation resistance. Machinability investigations so far have been intentionally focused on Ti-6Al-4V, which is commonly used in the aerospace research and development. However, a new classes of titanium alloys are also being developed for these applications. Ti-5Al-5Mo-5V-3C, also known as Ti5553, is included in this new category of titanium grade alloys. It corresponds to a near beta titanium alloy and generally it is employed on the production of high strength parts. Its high tensile strength combined with low weight (compared to Ti64) makes Ti5553 a suitable choice for landing gear parts and advanced structural components. However, due to the previously mentioned mechanical properties of Ti5553, machining processes can be difficult. During the cutting tests, the cutting zone experiences high cutting temperatures, and combined with a low rate of heat transfer, it generates stress and premature tool failure. By using several distinct experimental approaches, this work presents a comparison between different machining conditions (combinations of tools and coolants) to diagnose wear processes and identify better cutting parameters. The main objective of this research is to establish an understanding of how these parameters affect tribological aspects when machining Ti5553. The results of machining studies demonstrate different wear behaviour for CBN and

PCD tools under various cutting environments (different coolant modes). These operating conditions can considerably affect the cutting forces leading to an increased tool life and improved surface integrity by decreasing, the residual stress and roughness, as well as work of hardening the workpiece during machining operations.

ACKNOWLEDGMENTS

First and most importantly, praises and thanks to God, the Almighty, for His showers of blessings throughout my research work to complete the research successfully.

I would like to express my gratefulness to Dr. Veldhuis, who offered me the chance to work at the MMRI and provided me with all the required tools to carry out this study. In addition, I want to extend my sincere thanks to Dr. DePaiva and Dr. Fox-Rabinovich for their support and tutoring over the last two years. They also played a very important role in the realization of this mission. Moreover, I wish to demonstrate my sincere thanks to my laboratory colleagues who helped me with the analyses that made this work possible, as well as to all my professors who shared with me a portion of their expertise that is now being applied to this study. I would like to pronounce my thankful to Kennametal, in name of Dr. Joern Kohlscheen for all the support and sponsorship during my studies.

Finally, I would like to thank my partner, Djennyfer Kock, and my children, Sophie, and Theodore, who were with me and gave me their unconditional support on this trip, and my parents, who believed in my talent and invested deeply in my education.

CONTENTS

LIST OF FIGURES

LIST OF TABLES

NOMENCLATURE

Ti64 – Ti-6Al-4V

Ti5553 – Ti-5Al-5V-5Mo-3Cr

MMRI – McMaster Manufacturing Research Institute

ACARE – Advisory Council for Aviation Research in Europe

MRR – Material Removal Rate

HPC – High-Pressure Coolant

CP – Commercially Pure

HCP – Hexagonal Close-Packed

BCC – Body-Centered Cubic

UTS – Ultimate Tensile Strength

BUE – Built-Up Edge

MQL – Minimum Quantity Lubrication

TCCL – Tool-Chip Contact Length

SEM – Scanning Electron Microscopy

CNC – Computer Numerical Control

SE – Secondary Electron

V_p – Volume of peaks above reference

V_v – Volume of valleys bellow reference

PSDZ – Primary Shear Deformation Zone

SSDZ – Secondary Shear Deformation Zone

TSDZ – Tertiary Shear Deformation Zone

V_c – Cutting speed

DOC – Depth of Cut

SAC – Super Absorbent Coolant

1. Introduction

The production and improvement of different alloys is a constant process. In some cases, those new alloys offer a high resistance to further processing like machining operations. On the other hand, the machining industries seeking competitiveness, look for solutions that can result in high performance processes and cost reduction in compliance with the regulations and standards established for Aerospace's machined components. Since each new developed material is implemented in the industry, this will stimulate a desire for research studies in many associated fields. Data obtained from the production process of these new materials can serve to further develop effective applications, as well as improved products and processes.

1.1. Background

The challenges experienced by the aerospace industry during the last few decades are responsible for constant improvement and development in this sector. One example to explain how this economic sector plans years ahead is through the long-term strategic objectives outlined in by 'Flightpath 2050' [1] developed by the Consultative Council for Aviation Research in Europe (ACARE). These agreements put together ambitious goals for air traffic in 2050, which includes: (i) 75% CO_2 reduction per passenger kilometer; (ii) 90% reduction in NOx emissions; and (iii) 65% noise reduction.

This will require across-the-board improvements in the manufacturing of aircraft components. For instance, lighter materials for engines and structural parts, in addition to enhancements in aerodynamic design for lower fuel consumption.

As the consequence of their high strength-to-weight ratio, Titanium alloys are extensively employed in various applications in aerospace, automotive, chemical, and medical sectors [2]. As a result of their mechanical characteristics, those alloys are considered difficult to machine, this is due to their low thermal conductivity and high chemical reactivity [3]. Consequently, cutting tools experience several wear mechanisms, therefore, reducing a cutting tool`s life [4]. In addition, other properties such as low elastic modulus negatively affect the machining performance of these materials as well [5].

1.2. Motivation

Previous research typically focused on the application of coatings on the cutting tools to mitigate the extreme interactions that occur when machining titanium [6]. The outcome, however, have been so far unsatisfactory since most of the available coatings consist of Ti and Al which interact with the work material composed largely of a Ti. As an alternative solution to minimize thermal and mechanical stresses during machining, cutting fluids can be applied, particularly when operating at elevated cutting speeds, where high temperature is the major cause of aggressive tool wear rates [6], [7].

A comparison of specific process conditions of Ti5553 turning may produce useful information for further study.

To obtain reliable results, it is necessary to identify the best tooling system, which can deliver the longest tool life and best surface integrity (smoother surface topography, lower residual stress, and better cross-section hardness distribution).

During the machining of Ti5553 alloy, the shorter tool life is a direct consequence of severe tool wear. This is biggest issue when performing cutting operations on near-beta Ti alloys. As the main motivation for this work, and to comprehend the influence of different cutting conditions (tools and coolant modes) on the effect of the surface integrity, this study provides a number of experimental results and new findings that supports to establish a correlation between flank wear and the respective procedures in high-speed machining of Ti5553 alloy assisted by different cutting environments (dry, flood, high-pressure coolant, minimum quantity lubricant, and super absorbent coolant).

This study also seeks to outline an alternative method of improving productivity and reducing the cost related to the machining operations, by ensuring the surface integrity of the machined parts.

1.3. Research Objectives

The main purpose of this study is to provide to the existing knowledge of the machining of Ti5553. This work proposes a machinability study involving different cutting tools materials and different coolant modes to analyze differences in wear performance. A better understanding of these mechanisms related to the tribological aspects during machining will set the foundation for upcoming optimization strategies. This work could also serve as a guide for selecting tooling and machining parameters for the finish turning of aerospace titanium parts. The specific research objectives in this work are described as follows:

- Investigate the main wear mechanisms during machining of Ti5553 under different coolant conditions and evaluate their effects caused on the surface integrity of the machined workpiece.

- Identify the best interaction tool/coolant system, which will result in longer tool life and the best achievable surface characteristics (surface integrity) of the machined part (smoother surface topography, lower residual stress, and better surface hardness distribution).

- Provide a solution to improve productivity and cost reduction of the machining process, that follow the requirements related to surface integrity of the machined part.

1.4. Thesis outline

This thesis is separated into six chapters, which are briefly described as follows:

CHAPTER 1 – INTRODUCTION: The motivation and the primary research objectives of this research are presented in this chapter.

CHAPTER 2 – LITERATURE REVIEW: All major concepts, theoretical references and other relevant studies are presented in this chapter to provide sufficient background for this research. This chapter can be separated into four main points: the material (titanium alloy), the cutting tools, wear mechanisms and coolant system.

CHAPTER 3 – EXPERIMENTAL PROCEDURE: The methodology, experimental setups, test parameters and sampling are detailed in this chapter.

The experimental procedure is separated into three parts: workpiece characterization, cutting tests and surface integrity evaluations.

CHAPTER 4 – RESULTS AND DISCUSSION: The experimental results obtained in this research are presented and assessed in detail.

CHAPTER 5 – CONCLUSIONS: In this chapter, the main conclusions of the research will be stated based on the results achieved during the experiments.

CHAPTER 6 – SUGGESTIONS FOR FUTURE WORK: Based on the results achieved in this study, other related aspects are recommended for future study.

2. Literature review

2.1. Titanium Alloys

Titanium is present in 0.6% of the earth's crust and it is the fourth most common structural metal. A geologist called Reverend William Gregor discovered titanium in 1790. In order to obtain Titanium, two distinct minerals are extracted from the earth, commonly named as Ilmenite ($FeTiO_3$), and rutile (TiO_2) [2].

Soon after, a German chemist called Martin Heinrich Klaproth identified a dioxide of the same metal (TiO2) and named it after "Titanium.". He was unable to separate the metal [3]. and a commercially viable method was only developed around 1937-1940 by Wilhelm J. Kroll [2]. In the late 1940s, titanium gained widespread industrial significance thanks to its physical and mechanical properties and alloying characteristics [5].

Compared to other lightweight structural materials that are applied on the aerospace, automotive, chemical, and medical industries, the mechanical, thermal, and chemical properties of titanium qualify it for a wide range of applications. Another important characteristic of this material is its high melting point which provides good stability in terms of mechanical properties, when the service temperatures are high. [2], [8]. Overall, the titanium's main properties are strength retention at high operating temperatures, high strength-to-weight ratio, and relatively low elastic modulus including high corrosion and fatigue resistance [9].

Different titanium alloys are applied in the aerospace industry. For example, Ti-6Al-4V, or the Ti-5Al-5V-5Mo-3Cr (known also as a near beta alloy) are the main alloys applied in this segment. Both offer desirable properties that are considered suitable materials to be employed into two categories: frames and engines.

The demand for β titanium alloys in the aerospace industry is increasing [2], [10]. These alloys present attractive mechanical properties for structural aircraft components such as aero frames and landing gears components. Its characteristics will be discussed in the next section.

2.1.1. Classification of Ti Alloys

Titanium alloys can be characterized as presenting an allotropic phase transformation at 880ºC [2], [6], [11]. At lower temperatures, the microstructure consists mainly of HCP (Hexagonal Close-Packed) crystals, also known as α phases. Upon reaching a recrystallization temperature (860ºC), the crystallographic structure changes to a BCC (Body Centered Cubic) shape, also called as beta phase [2], [11]. Nevertheless, this exact temperature of transformation can only occur for 100% pure titanium samples. The presence of other stabilizing components determines the dominant phase of the titanium alloys. As shown in Figure 1, elements such as molybdenum and vanadium support a crystallographic structure of the BCC, whereas aluminum and carbon serve as α-stabilizers, which make HCP predominant [2], [4]. These compositions directly affect the material's capability to obtain optimal tensile resistance (UTS) and hardness (H) after aging.

Figure 1 presents the phase diagram and the positions of each of the alloys studied in this work.

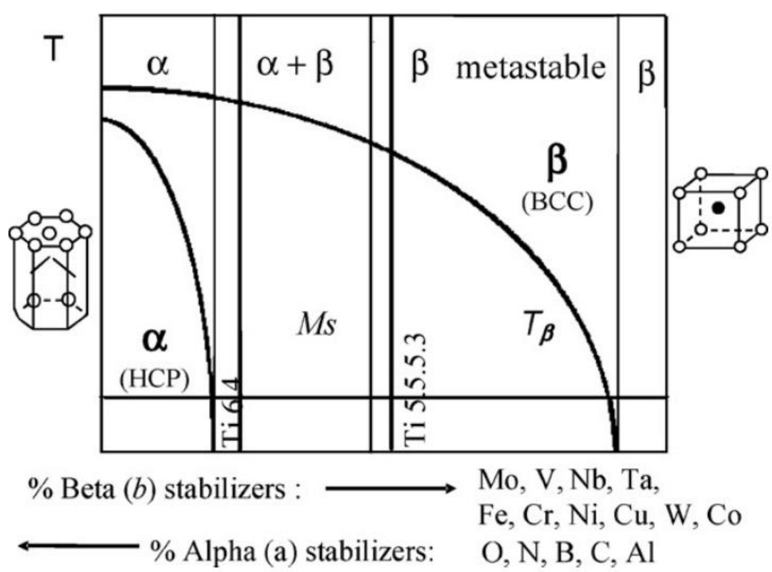

Figure 1: Titanium phase diagram [9]

Although α Titanium alloys have lower mechanical characteristics, their corrosion resistance is superior to that of β alloys [12], [13]. Near-β alloys consisting of a β matrix with α precipitates possess high mechanical resistance characteristics of the β process combined with α alloy corrosion properties [14].

2.1.2. Ti-6Al-4V

Ti-6Al-4V (Ti64) is by far, the most commonly used α+β titanium alloy with the application range comprising 45-65% of the titanium consumption around the world [2]. In comparison to other titanium alloys, such as near-α and β, Ti64 provides a good balance of strength, ductility, fracture durability, processability, resistance to corrosion and weldability, as well as hardenability and heat treatment capacity. Due to its moderate heat resistance, Ti64 is extensively used in the aerospace industry, particularly among structural engine components operating at temperatures of up to 300^{o}C. The alloy's heat resistance is highly dependent on its β content [4], [15].

Possibly the greatest factor favoring the use of Ti64 is the wide variety of available knowledge regarding its treatment (annealing, quenching, aging) and processing methods, since the application of this alloy have been already widely explored in industrial research over the years [16]. Table 1 and Table 2 describe the structure and mechanical properties of this alloy under study.

Table 1: Chemical composition of Ti64 [9].

Al	V	Mo	Cr	Fe	Zr	C	O
5.5-6.75	3.5-4.5	--	--	~0.4	--	~0.1	~0.2

Table 2: Mechanical properties of Ti64 measured at room temperature [9].

Yield strength (MPa)	Tensile strength (MPa)	Elongation (%)	Hardness (HV)	Thermal conductivity (W/m.^{o}C)	T_{melt} (^{o}C)	Heat Transfer
828	895	10	360	6.6	1630	

As demonstrated, due to these properties, the Ti64 is several aerospace industry applications.

2.1.3. Ti-5Al-5V-5Mo-3Cr

The Ti-5Al-5V-5Mo-3Cr or Ti5553 contains only 20% of the α phase, it is known as a near-β alloy (β metastable) [4], [6], [7], [9], [13]. Ti5553 has a similar Young modulus to Ti64, according to previous findings [9]. However, these materials are substantially different from a mechanical standpoint, with Ti5553 having a 30% higher yield and ultimate tensile strength and significantly lower ductility [9]. The concentration of Mo present in Ti5553 is significantly higher (approximately eight times) than that of Ti64, which partially accounts for its superior resistance to tensile load [9]. Both properties benefit the material's ability to endure greater workloads. On the other hand, these characteristics of Ti5553 result in poorer machinability when compared with Ti64 [9], [17].

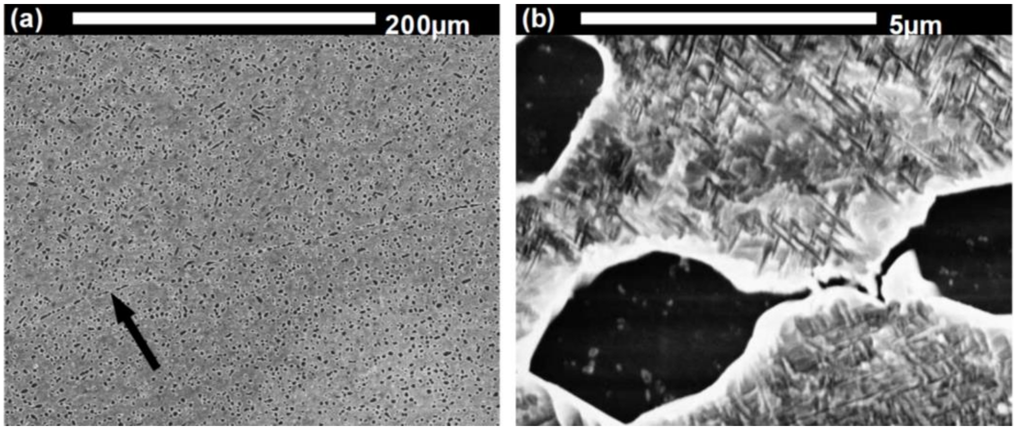

Figure 2: SEM images of surface of the received Ti5553 alloy. (a) general view with prior β grain boundary (arrow), and (b) magnified view of α precipitates on the β grain boundary [3].

The composition and measured mechanical properties of Ti5553 are presented in Table 3 and Table 4.

Table 3: Chemical composition of Ti5553 [9].

Al	V	Mo	Cr	Fe	Zr	C	O
4.4-5.7	4.0-5.5	4.0-5.5	2.5-3.5	0.3-0.5	0.3 max	0.1 max	0.18 max

Table 4: Mechanical properties of Ti5553 measured at room temperature [9].

Yield strength (MPa)	Tensile strength (MPa)	Elongation (%)	Hardness (HV)	Thermal conductivity (W/m.ºC)	T_{melt} (ºC)	Heat transfer
1170	1290	6	415	5.0	1650	

Owing to previously described hardenability, it is possible to manufacture, and heat treat components with broad dimensions. Based on that, understanding the machinability and wear mechanisms of this material is an important factor when developing cutting tools. In the next section, the machinability aspects of Ti5553 are described.

2.1.3.1. Machinability

Very limited research has been done with regards to machinability of these alloys. Arrazola et al. [9] performed a comparative study on the machining of Ti5553 (near β) and Ti64 (α+β) titanium alloys. Based on this analysis, the machinability of the Ti5553 alloy is approximately 44% lower compared to the Ti64 alloy (the reference material).

While the wear mechanisms in both alloys are similar, the strength of Ti5553 is significantly higher, and this affects the cutting process [9].

Moreover, several studies investigated the effect of the temperature generated into the cutting zone. As results of this studies, the temperature collected during the turning of Ti5553 show a substantial increase of the heat generated at the tool/chip zone. This was observed while there was only a slight increase in temperature at the primary shear deformation region [18]. This can be attributed in reason of the reduced thermal conductivity that Ti5553 posses [4], [9], [19]. Analytical modeling and experimental investigations confirmed that an inverse relationship exists between temperature and friction coefficient on the rake face of the tool as a consequence of the accumulation of work material in the form of a build-up layer on the tool [9], [20].

Another study carried out by Nouari et al. [21] considered orthogonal cutting tests. Found that the chip formation process is also related to the poor machinability of this alloy. The presence of high-frequency adiabatic shear bands could lead to variations in cutting and feed forces, which are considerably higher in the near-β alloy [22]. Furthermore, this study found that Ti64 alloy is more susceptible to thermal softening, whereas Ti5553 alloy is more vulnerable to work hardening. According to the authors, the adhesion and diffusion are the primary tool wear mechanisms. Consequently, the cutting forces for the Ti5553 are 20 to 40% stronger (this relation is dependent of the rake angle of the tool). When machining the Ti5553, the main wear mechanisms that the cutting tool is exposed are abrasion, diffusion, and adhesion. Additionally, its lower machinability can be attributed to higher cutting temperatures and mechanical properties, chip segmentation frequency and adhesion tendency.

Overall, the machinability of Ti5553 follows the general trend of Ti alloys, which are generally considered hard-to-cut material (low machinability) and it is inherent to its composition and properties. Ti5553 is also highly chemically reactive, and as a result, the material shows a tendence to adhere on the rake face of the cutting tool while the cut is performed. The negative effect of this phenomena it is the occurrence of chipping and this is results in reduced tool life period. As a response of the material`s low thermal conductivity, high temperatures at the tool / workpiece interface occurs and this collaborates to reducing tool life. In additional, the material`s low machinability it is also attributed to its high strength, low elasticity modulus and high temperatures [23]. Siekmann said in 1955 that "the cutting process of titanium alloys will continue being a challenge, no matter what of the methods applied to develop the cut of this metal" [24]. Based on those challenges faced during the machining of Ti5553 several companies have been investing heavily in the development of procedures and methods to enhance the machining process of this alloy and consequently decrease the machining cost.

2.2. Materials for cutting tools.

For many years, tool materials for cutting applications have been developed with new tool materials being found to meet the requirements presented by the introduction of new materials considered hard- to-cut [6].

Currently many tool materials are available like High Speed Steel, Carbide, Cubic Boron Nitride, Poly Crystal Diamond tools that have demonstrated value in meeting specific requirements such as: the capability of achieving acceptable performance in several of applications, satisfactory tool life, and high metal removal rate, surface finish, at a reasonable cost [7].

Figure 3 illustrates a timeline of significant advances in tool materials from 1900 to 1980. Figure 3 includes only those objects that seem to have a long (100-year) future.

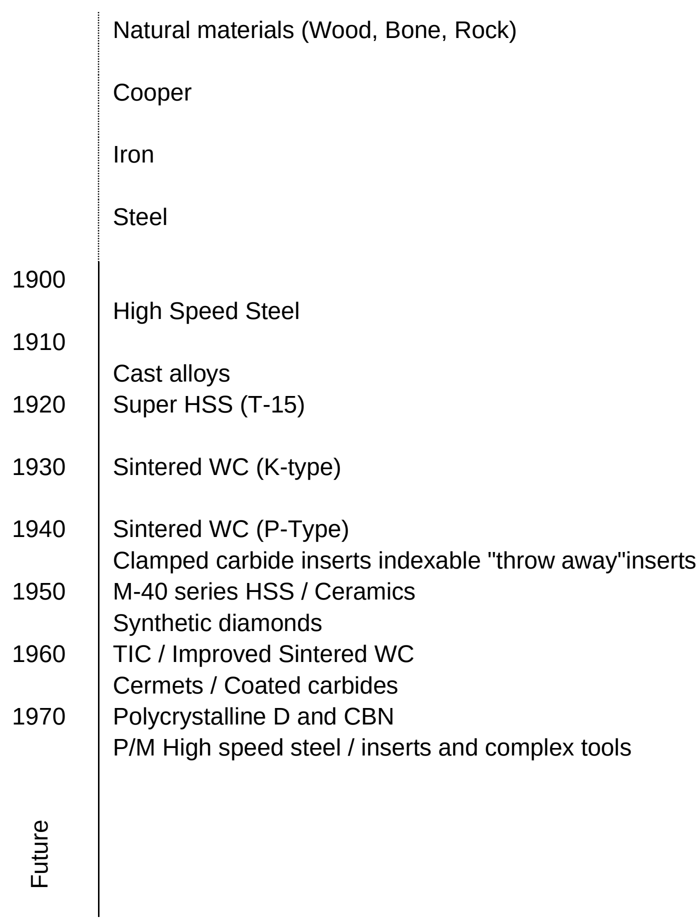

Figure 3: Approximate dates for the introduction of different cutting-tool materials [7].

The most remarkable aspect is the rising scale at which new concepts have been developed since 1900. This was due, in part, to the rapid advancement of material science and, this case to the demand for unique machining features. [7].

2.2.1. Carbide

Tungsten carbide is one of several compounds comprising transition elements. These materials are significantly used as tool materials and they hold a dominant position as the major material for cutting tools driven by the composition of tungsten carbide [6].

Tungsten and molybdenum carbides have hexagonal structures. Major structural changes do not occur in these stiff and strongly bonded compounds; therefore, heat treatment or high temperature do not alter their properties. At extreme temperatures, the resistance of carbides decreases rapidly, but they remain much more resistant than steel in almost all circumstances. The use of carbide cutting tools is encouraged by its hardness and properties' stability in under a wide range of heat treatments [7].

The powder metal production process allows precise control the carbide grains size as well as the chemical composition of the alloy [6]. Figure 4 demonstrates how the tungsten carbide is assembled on the binder.

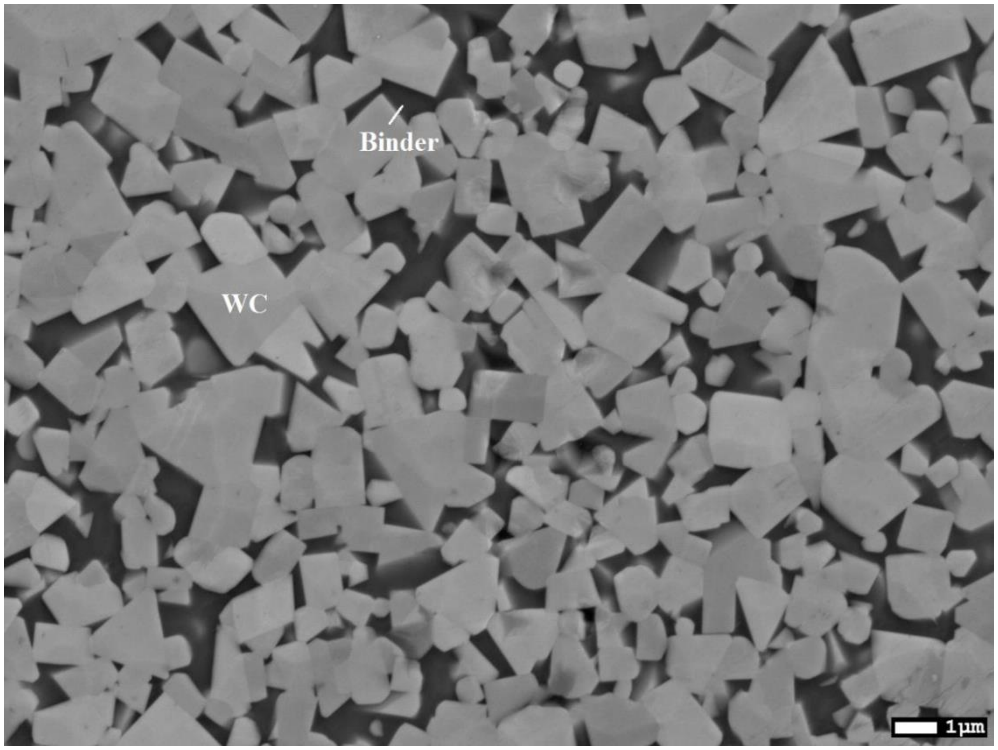

Figure 4: Cemented carbide - The "Cobalt binder distribution into the cemented carbide" grain size differs following the HW grade application [11].

Table 5 shows the classification of carbides corresponding to use.

Table 5: Carbide classification [15].

Symbol	Category	Color code	Designation
P	Ferrous metals with long chips	Blue	P01
			P10
			P20
			P30
			P40
			P50
M	Stainless steel / Cast Steel	Yellow	M01
			M10
			M20
			M30
			M40
K		Red	K01

	Cast Iron (Gray cast iron / Nodular cast iron)		K10
			K20
			K30
			K40
N	Nonferrous metals (Aluminium / Nonferrous metals / Non metals	Green	N01
			N10
			N20
			N30
S	Hard to machine materials (Titanium alloys / Heat-resistant alloys)	Brown	S01
			S10
			S20
			S30
H	Hard materials (Hardened steel / Chilled cast iron)	Black	H01
			H10
			H20
			H30

According to Table 5 the cemented carbides tools present a combination of high strength and elevated hardness by the capacity to bend plastically under compressive stress before failure (toughness). These characteristics make the cemented carbides a suitable material for use as cutting tools.

2.2.2. CBN

The CBN cutting tool is also technically known as Polycrystalline cubic boron nitride. This cutting tool is manufacturing by powder metallurgic, where the CBN grains are sintering with a binder material, and it became a very attractive material to be applied as a cutting tool material that can overcome some difficulties found during machining of hard-to-cut materials. These cutting tools have a few desirable mechanical and physical properties. Its properties offer high thermal conductivity, and good thermal stability [6].

CBN tool is considered a material with high hardness been close to the diamond [25], [26]. For this reason, there is an extensive list for applications of polycrystalline cubic boron nitride as a cutting tool material for machining hard-to-cut alloys. Additionally, these cutting tools offer excellent hot hardness enabling this material to be employed at very high cutting speeds. It also exhibits good thermal shock resistance and good toughness [27].

The microstructures of CBN tools are shown in Figure 5. The overall distribution of coarse grains is relatively uniform but there are still some binder agglomerations Figure 5a shows that the microstructure distribution of fine grains is unbalanced, and Figure 5b shows an example of a sample with a high amount of binder agglomerations [27].

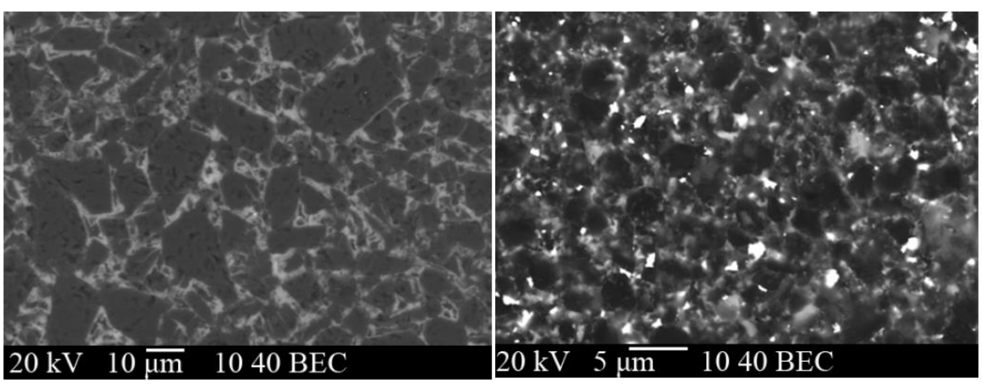

a) Grain size 6-22 µm   b) Grain size 1-4 µm

Figure 5: Two grades of the CBN tool microstructures: (a) 6-22 µm grain size (binder B, N, Al) (b) 1-4 µm grain size (binder B, N, Al, Ti, Co, W) [28].

The material hardness changes with the surface direction, which is induced by the crystal lattice's relative distribution that can variate from 40 to 55 GPa. This hardness is significantly higher than metallic carbides. [6].

The literature reports a large number of tool wear studies involving CBN. These were preformed in an effort to find better processing conditions and suitable applications taking into account the tool wear pattern and wear mechanism perspectives. In this research, CBN cutting inserts have been selected as the material of choice for the studies performed in this research [7].

2.2.3. SiAlON

Sialons (Si-Al-O-N) are prepared of silicon nitride materials with addition of fractions of oxygen and aluminium. Silicon nitride (Si_3N_4) has valuable properties. For instance, a low thermal expansion coefficient (3.2 x 10^{-6}), high hardness (approx. 2000 HV) and better bend strength than aluminium (approx. 900 MP), providing thermal shock resistance [6].

Most of these tools are produced of finely divided sintered α-aluminum without the use of additives or binders. Ceramic tools are, in majority, tougher and more refractory materials than carbide tools, but they are still far more fragile. To provide acceptable strength, aluminium oxide tools must have a specific range of grain sizes and should be sintered for maximum density [7]. The Figure 6 shows an example of the size of grains typical of this material.

Although the cost of aluminium oxide used to manufacture ceramic tools is low, the cost of processing is high, this is mostly due to the need to cut large blocks into small parts using diamond saws. Ceramic tools have been shown to be of great value in the manufacturing of cast iron and hardened steel components [6], [7].

Since ceramic tools are brittle, they easily chip when machining soft steels specially if the cutting conditions produce a large unstable built-up edge (BUE) or for discontinuous cuts. Ceramic tools show reduced tool life especially when applied during machining of aluminium or titanium alloys due to oxidation of the surface (high affinity between these metals with oxygen). When machining these materials strong bonds are formed between the chip and the tool, and the tool's wear rate is then accelerated [7].

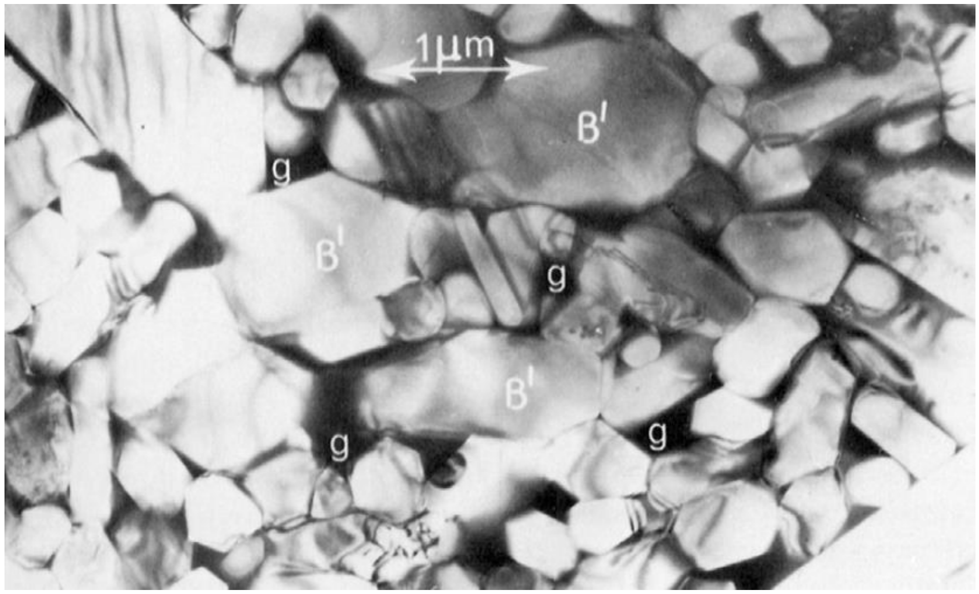

Figure 6: TEM images revealing the as-sintered structure of sialon containing yttria addition: β´ represents Si_3-N_4- based phase with substituted Al and O; g is the glassy phase [6].

2.2.4. PCD

Polycrystalline Diamond or PCD is one of the hardest and most abrasion resistant tooling material available in the market and consists of diamond particles (diamond grit) which are sintered together with a metallic binder (cobalt). But the high cost of these materials has limited its use to applications where other tool materials cannot work successfully. As a result of diamond's very high hardness it performs well in cases where abrasion is the prevailing wear mechanism. As such all forms of PCD tools display a much lower rate of wear and longer tool life than carbides or oxides [6], [7].

The crystal structure of diamond is responsible for its uniquely high hardness. Two interpenetrating cubic lattices are configured face centered in a way that each carbon atom has four close neighbors connected by co-valent bonds. The hardness and resistance of any surface to abrasive wear depends significantly on the alignment between the surface in relation to the crystal lattice [7].

Single crystal natural diamonds have been used in many industrial applications. Large natural diamonds are suitable for cutting operations as single cutting edge in particular applications. The optimal orientation is chosen, and they are lapped and placed in tool holders of the appropriate shape for a cutting edge. The tool edges can be designed for shape and edge execution with extraordinary precision and can create surfaces with exceptionally high quality and finish [6].

The structures of two polycrystalline diamond tools are shown in Figure 7. Most tool tips that are commonly accessible are laminated heads. A sheet of polished diamond, normally 0.5 to 1 mm thick, is attached to a cemented carbide substrate, typically around 3 mm thick, to create a tool edge.

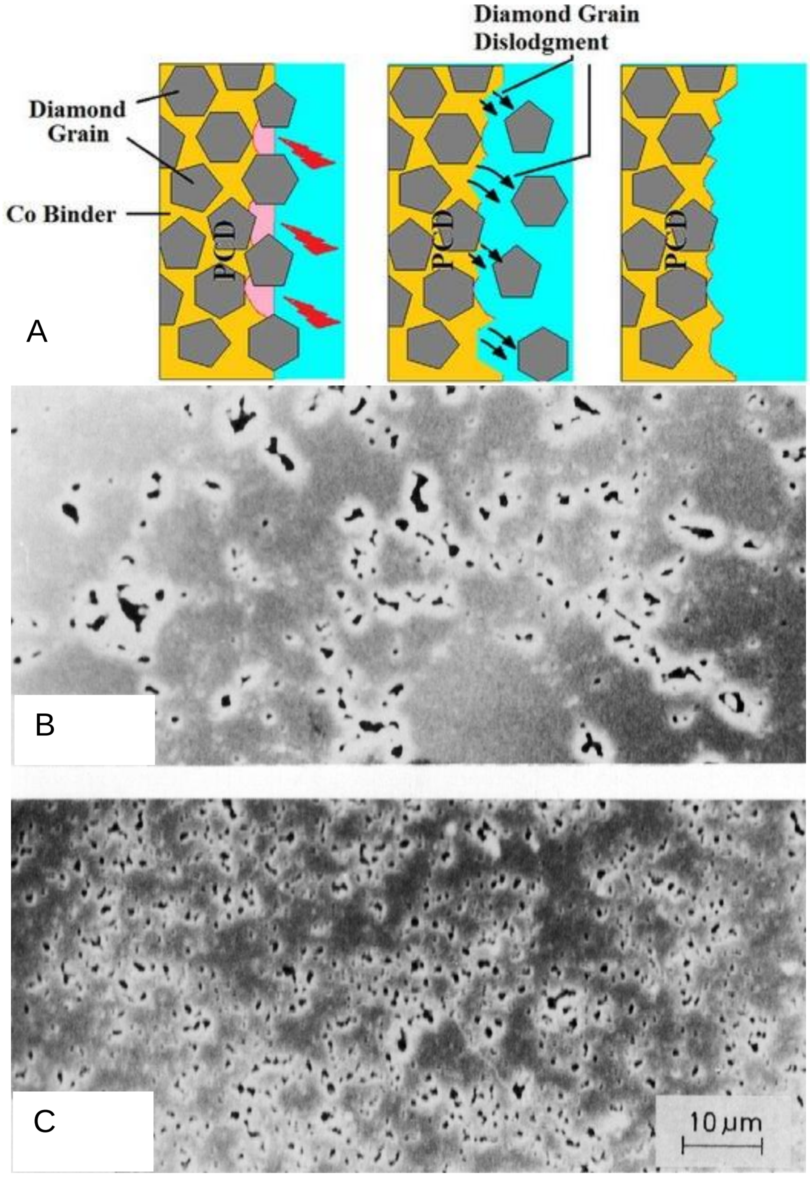

Figure 7: SEM images of two grades of PCD tools: (a) diagram of microstructure of PCD tool (b) 25 µm grain size (c) 2 µm grain size [6].

The Table 6 condenses important properties of different tool materials.

Table 6: Properties of several types of tools [6]

Tool material	**Transverse rupture strength (MPa)**	**Compressive strength (MPa)**	**Hardness (HV)**	**Fracture toughness (K_{IC})**	**Thermal conductivity at 20ºC (W/mºC)**
WC-Co 3% WC grain size 1.4 µm	1000	-	1820	8	-
WC-Co 6% WC grain size 1.4 µm	2300	4250	1575	10	-
WC-Co 9% WC grain size 1.4 µm	2400	4000	1420	13	-
Al_2O_3	550	3000	1600	4	10.5
Al_2O_3 / TiC	800	4500	2200	4.5	16.7
Al_2O_3 / SiC whiskers	900	-	1925	7	13.0
SiAlON (sintered)	800	3500	1870	6.5	20 – 25
PCD	-	4740	5100	8.8	560
PCBN	-	3800	3000	4.5	100

Considering the performance of the tools mentioned so far, this study is carried out to compare the different performances of a select number of tools when turning Ti5553. This research involves analyzing the different types of tool wear mechanisms commonly observed, which will be presented in the following section.

2.3. Wear Mechanisms

Throughout the machining process, the cutting tool is exposed to extreme mechanical and thermal stresses, which are generated based on the combination of the workpiece material and the cutting conditions selected to perform the machining. These stresses eventually result in wear or damage of the tool.

Wear is a progressive phenomenon on the tool's surfaces which is caused by the cutting action, and over time it changes the tool's shape and hence its original geometry which impacts the machining process.

Wear is the product of different mechanisms, where one mechanism can dominate over another. Depending on the part and tool material, the machining process, the cutting conditions, the tool configuration and cutting fluid applied during cutting [29].

The following section will present a general concept of the main wear mechanisms found during the machining process.

2.3.1. Abrasion

Abrasion wear is one of the major causes of damage to the cutting tool edge. Abrasion may produce wear on both the flank and rake face of the tool. When reporting wear, it is common to predominantly report flank wear. Flank wear develops as the clearance surface rubs against the component over time. Wear on the rake face can generate a crater as the tool chip slides over the surface of the tool.

The rate of abrasion wear is increased by the presence of hard particles in the material of the workpiece and by high cutting temperatures which effectively reduces the hardness of the cutting tool. Therefore, cutting tools with elevated hot hardness properties provide higher levels of resistance to abrasive damage and consequently provide better performance. Often, hard particles adhere to the surface of the tool and are dragged along the flank face as the cutting tool slides along the workpiece. In this case, abrasion typically takes place on the cutting tool flank face as is shown in Figure 8 [27].

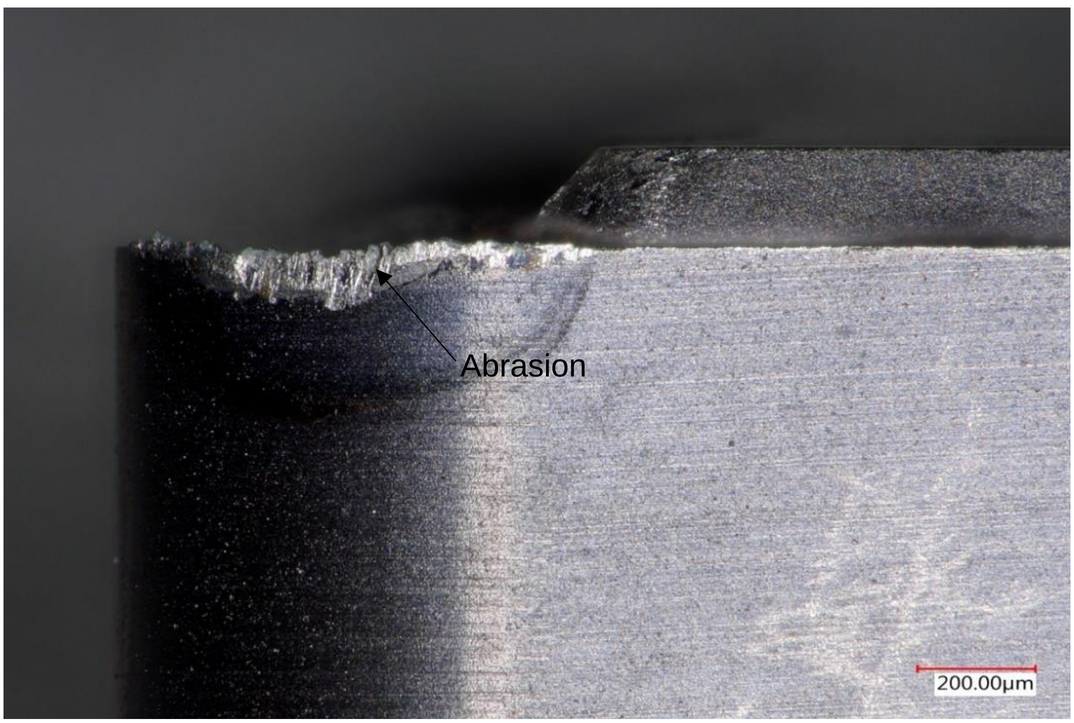

Figure 8: Abrasive wear on the Carbide tool.

2.3.2. Adhesion

Adhesion wear occurs when a fragment of the tool is removed from the surface on a microscopic scale. Then, because of the high temperature and pressure at the cutting edge, a metal bond forms in the tool/chip interface welding them together. The welded material leads to an unsteady chip flows over the rake face of the tool forming BUE. The chip flow over the BUE with time will result in fracture of the welded material and some of the tool material will be dragged out along with it by adhesion. Adhesion can be controlled by using a cutting fluid that can provide a film between the contact surfaces [29]. The Figure 9 shows adhesive wear.

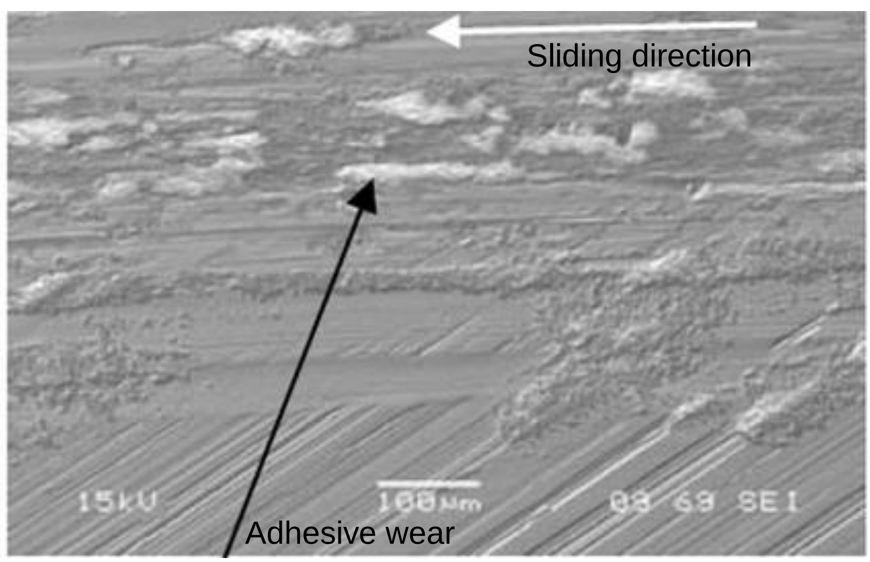

Figure 9: Adhesive wear [30]

2.3.3. Diffusion

The diffusion process is a phenomenon that is activated in the cutting zone by temperature. This phenomenon is usually a characteristic of a high-speed cutting operation. As a result of this process crater wear is observed on the rake face of a cutting tool. Figure 10 shows a worn tool with a typical tool wear pattern which is generated by diffusion. Solid-state diffusion consists of transferring the atoms from one metal to another. The rate of diffusion depends on the temperature of the two metals involved, and the duration of the contact, and the physical-chemical affinity between the respective materials. As it is done at the atomic level, the areas worn by diffusion have a smooth appearance when viewed under the microscope [11].

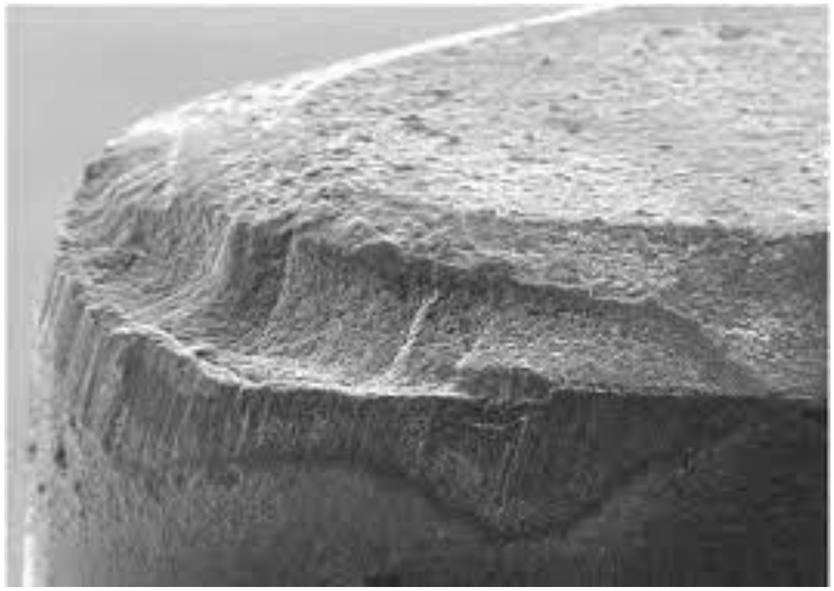

Figure 10: Diffusion [11]

2.3.4. Oxidation

The chemical reaction between the surface of the tool in an area of high temperature and in contact with oxygen results in a process called oxidation. In this process, a layer of oxides is formed on the surface and, when abrasion is removed, another layer is formed during the machining process [27].

This is a repetitive process of oxide layer formation and removal. In some special cases this slight build up layer helps to reduce tool wear by isolating the tool and the workpiece and providing the contact zone with unique properties [31].

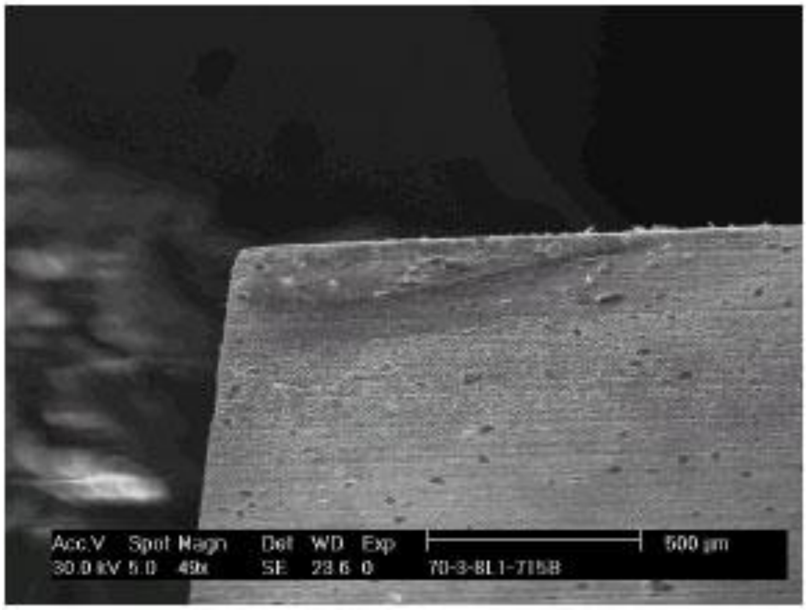

Figure 11: Mechanism for the formation of oxidation [15]

2.4. Coolant Systems

Various methods have been introduced to enhance machinability in order to improve production processes. For example, to reduce the inherent heat generated during cutting operations, coolant is applied and acts by reducing friction between the tool and the workpiece and consequently aiding in material removal. The application of cutting fluids is also a way to improve the surface roughness of the final products [29].

Overall, the role of cutting fluids is to cool and lubricate the cutting zone during the machining process. As a result, the tribological conditions between the tool, the chip, and the workpiece can be improved; the temperature in the cutting zone can be stabilised (reducing fluctuations in temperature and reducing heat generation); and chip removal can be facilitated. [29].

Different methods of fluids application during machining processes will be discussed in detail on the following sections.

2.4.1. Flood

Flood Cooling is an optional system that is generally implemented on higher-end CNC machines. A constant flow of coolant is applied through the nozzle targeted at the workpiece or at the tip of the cutting tool. The coolant can be recovered through a recovery basin located under the machine bed. The steady flow of coolant removes cut chips and keeps the cutting tool cool and well lubricated [7].

Currently, there is less focus on the use of flood coolant techniques for machining purposes as traditional cooling methods are in disagreement with new environmental restrictions and health practises [32]. New techniques to flood cooling are being employed to reduce the costs associated with purchasing and disposing of cutting fluids and their environmental and health impacts. As a result of this trend, new cooling, and lubrication technologies such as minimum quantity lubrication (MQL), and nanofluid are gaining popularity. However, in spite of the promising characteristics that many investigations have reported on the use of these methods, there are some shortcomings to their practical application in industry related to chip evacuation and mist containment [33].

2.4.2. High Pressure Coolant (HPC)

The use of cutting fluids to improve tribological conditions is a widely used technique for machining materials with low thermal conductivity, especially at higher cutting speeds, where the primary cause of accelerated tool wear, is the heat generated [5]–[7]. However, traditional coolant supplies do not guarantee that the fluid will be targeted at the cutting zone due to the sticking-sliding nature of the chip formation process [7], thus conventional coolant application does not achieve significant efficiency in terms of penetrating into the cutting zone [34]. Cutting fluids are directed at the primary (PSDZ), secondary (SSDZ), and tertiary shear deformation zones (TSDZ) with careful setup. The SSDZ (the tool/chip interface) is impacted by a combination of high shear and normal stresses that run parallel to the long tool/workpiece interface [6], [7]. Figure 12 shows the tree different shear zones.

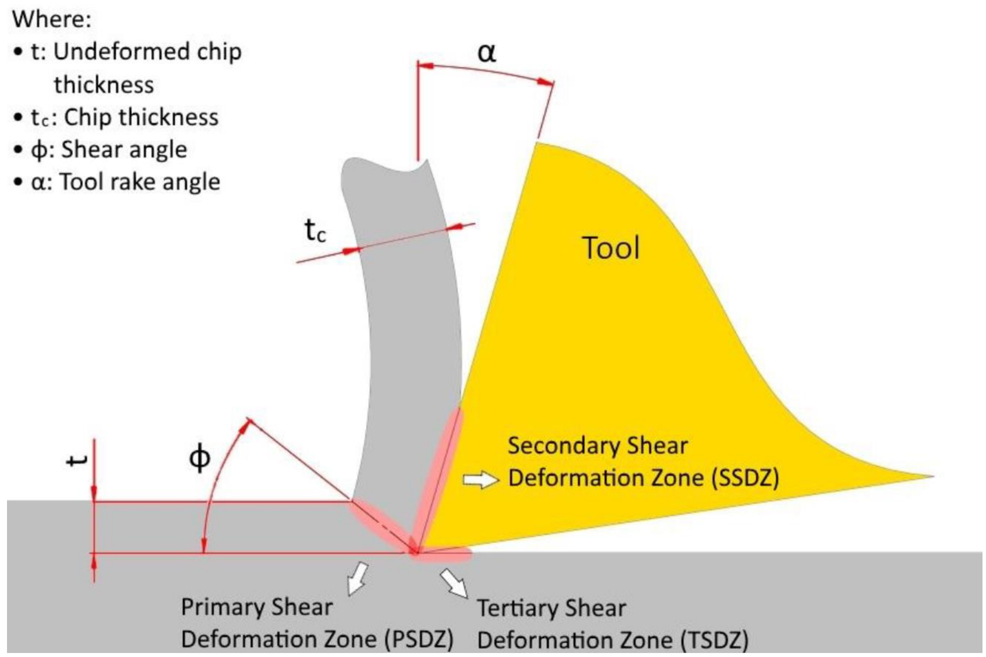

Figure 12: Primary, secondary and tertiary cutting zones schematics [7]

The SSDZ is the region that requires the most coolant action due to high temperature realized in this region during the cutting process. A vapour barrier can be created by the harsh tool/chip contact conditions making it hard for the flood coolant supply to adequately access the secondary shear deformation zone, thus, preventing heat exchange between the cutting fluid and the cutting insert. Different cooling approaches have been used to solve this issue and enhance the machining performance of titanium alloys [35].

The use of HPC is an emerging solution which can provide a relatively low-cost alternative capable of addressing the majority of the previously mentioned issues [34], [36], [37]. Also when machining Ti alloys, HPC improves sub-surface integrity of the workpiece [34]. The main advantages of applying HPC to the rake face of the cutting tool are illustrated in Figure 13. Its possible to observed the chip curl reduction increasing the chip breakability from the additional bending moment that is being applied, and more effective heat dissipation from the tool/chip interface, since the coolant can reach deeper into the cutting zone [7]. Lower diffusion wear rates due to the shorter Tool/Chip Contact Length (TCCL) extends the cutting tool`s service life [7].

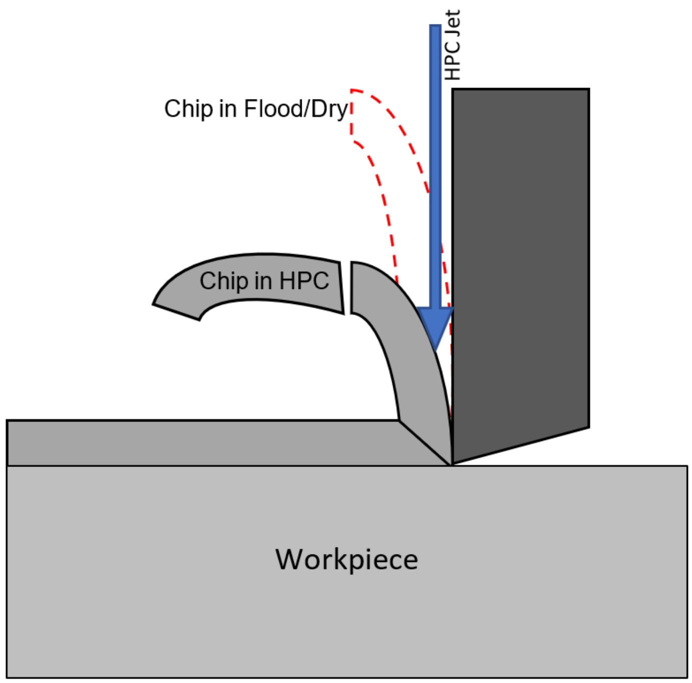

Figure 13: Using HPC in the rake face.

2.4.3. Minimum Quantity Lubrication (MQL)

Changes in environmental awareness increasing cost and pressure imposed by industrial investors has resulted in crucial concern of traditional cooling lubricants applied in machining operations. Depending on the workpiece, the production size and location, the costs associated with using cooling lubricants vary from 7 to 17% of the total production cost. By abandoning conventional cooling lubricants and using dry machining or MQL technologies, this cost factor can be significantly reduced [38].

In addition to increasing the productivity of the manufacturing process, such technical advancements help to protect workers and the environment. The reduction of substantial exposure to cooling lubricants at work enhances employee satisfaction while also improving work efficiency [38].

2.4.4. Super Absorbent Coolant (SAC)

A Super Absorbent Coolant (SAC) is created by the uniform distribution of solid nanoparticles within a fluid. SAC can be designed to have a high thermal conductivity and lubricity compared with regular fluids. They are utilized in a large selection of applications such as engine cooling, water heating with solar energy, chillers and manufacturing processes. The purpose of applying SAC in machining is to use the mobility of nanoparticles to better penetrate the cutting zone and use materials with high lubricity to decrease the friction between surfaces in the cutting zone [33].

Figure 14: SAC delivery system

2.5. Research Gaps

Considering the topics explored in this literature review, there is a demand to understand different aspects related to the machine of Ti5553. The following gaps are identified:

1. There is limited related research outlined in the literature regarding selecting the best tool material for machining Ti5553.

2. Finding the best cutting strategies (cutting parameters and lubrication modes) to improve tool life, considering aspects of the integrity of the surface used.

3. Identify the main mechanisms of wear related to the use of the different cutting strategies used in this work.

3. Materials and Methods

This section will describe the selected materials and the designed methods to develop the research studies. Initially the workpiece characterization was performed, which consisted of an examination of the material's microstructure. The following section (experimental procedure) will present the methodology and the equipment employed to run several machining operations. After that, surface integrity studies were performed on the machined surface by the selected cutting procedures, evaluating surface texture, hardness, and residual stresses.

3.1. Workpiece characterization

The material used in this work was Ti5553 produced by Grandis Titanium. The material's chemical composition provided by the manufacturer is displayed in Table 7.

Table 7: Chemical composition of Ti5553 (Grandis Titanium)

Element	Mo	Zr	Fe	V	Si	Al	C	O	N	Cr	Y
Max % Min	5.01 – 4.99	0.002	0.35	5.07 – 4.95	0.03	5.44 – 5.38	0.020 – 0.017	0.13	0.009 – 0.008	2.92 – 2.88	< 0.0004

To evaluate the Ti5553's microstructure a sample cross-section was prepared taking into account the axial direction of the material, then, mounted in epoxy resin and metallographically prepared using conventional methods and etched in a solution of 2% Hydrofluoric acid revealing its microstructure. To collect microstructural images an optical microscope Keyence VHX-6000 was used. The respective microstructures can be seen in Figure 15.

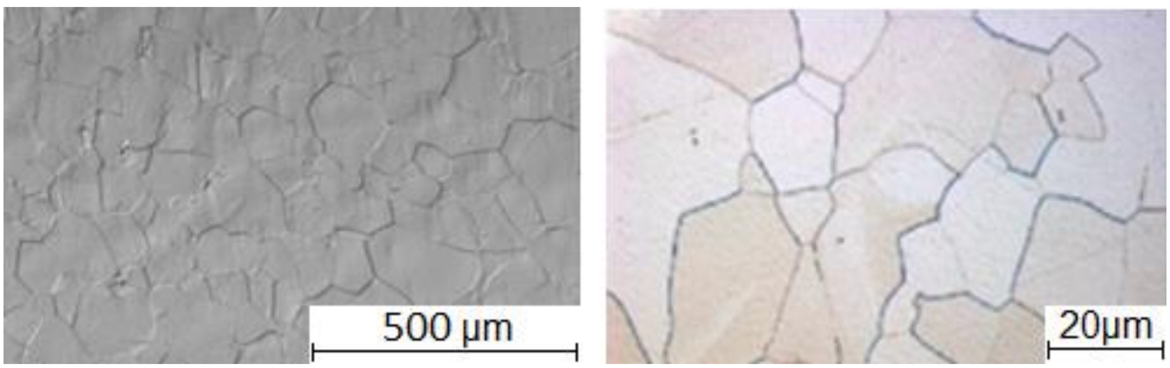

Figure 15: Microstructure of Ti5553

3.2. Experimental procedures – cutting tests.

The experimental methodology used in this study is presented in this chapter. A schematic model outlining the steps of the experimental procedure is shown in Figure 16.

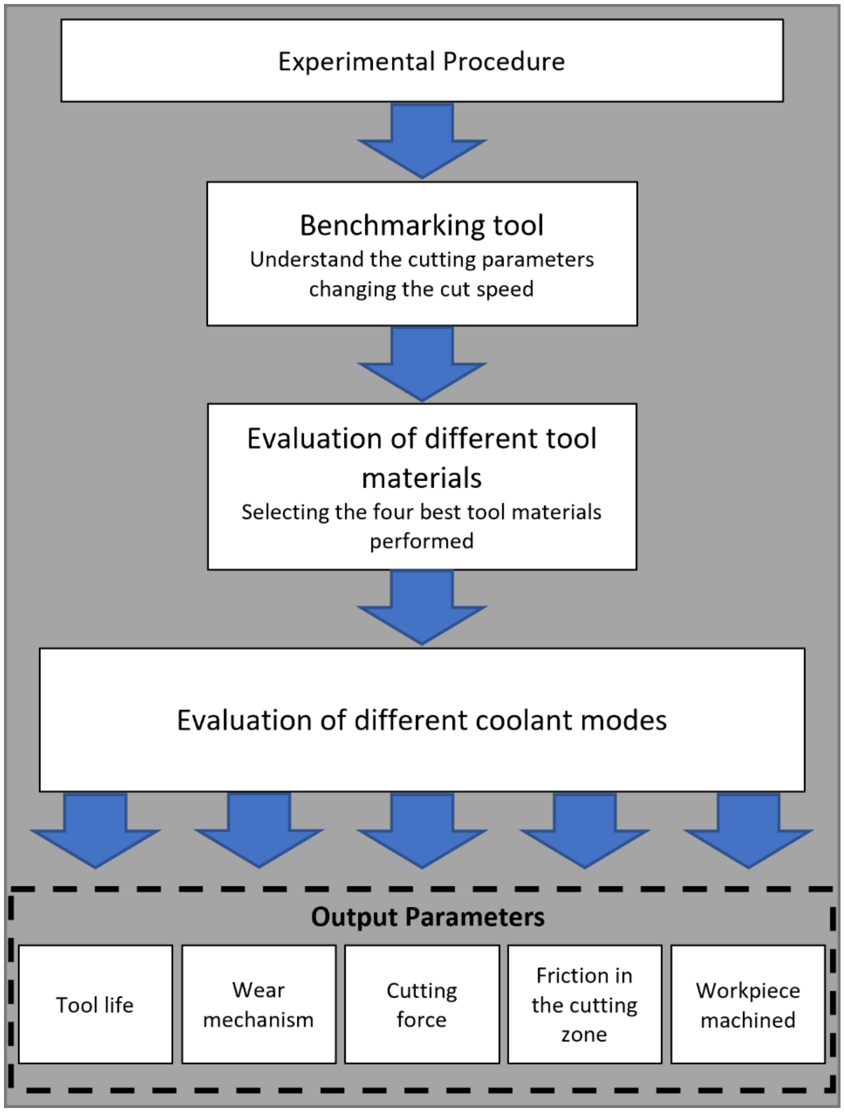

Figure 16: Experimental plan schematics

During this stage, tool life, cutting forces, and wear analysis were collected under different coolant modes applied to assess the best tribological conditions that can be achieved in the cutting zone. The following individual stages described below will provide a very detailed plan of each stage presented on Figure 16.

- Benchmarking tool - SC-450 Nakamura Tome CNC lathe (Figure 17a) was used to perform the cutting test. Different cutting speeds (120, 250, and 400 m/min) were applied to establish the ideal cutting conditions to promote a reasonable curve for the tool life. The feed rate (f) and depth of cut (DoC) were kept constant at 0.1225, and 0.25 mm, respectively. The geometry of the cutting inserts is commercially available and were supplied by KENNAMETAL (according to Table 8). The cutting tools were assembled in the Kennametal DCLNL123BKC3 tool holder (Figure 17c).

Table 8: Applied tools.

Number	Grade	Corner image	ISO catalog number	Substrate	Coating
WCO1C1	KCU10		CNGG120408FS	Carbide	PVD multilayer
WCO1U	K313	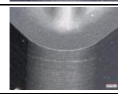	CNGG120408FS	Carbide	Uncoated
WCO1C2	KC5010		CNGG120408FS	Carbide	PVD AlTiN
CBN1U	KB1630		CCGW120408S01015M	CBN	Uncoated
CBN1C	KB5630		CNGA120408S01025M	CBN	PVD AlTiN
SIA1U	KYS30	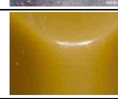	CNGA120408E	SiAlON	Uncoated
SIA2C	KYS25		CNGA120412T01020	SiAlON	CVD Alumina-TiCN
SIA3U	KY1540		CNGA120412T01020	SiAlON	Uncoated
SIA4C	KY4300	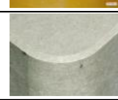	CNGA120408T01020	SiAlON	Matrix Al_2O_3+SiCW
PDC1U	KD1425	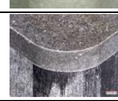	CNMS120408FST	PCD	Uncoated
PCD2U	KD1400		CNMS120408FST	PCD	Uncoated

The machine setup as well as the tool holder dynamometer (three-component Kistler 9121) employed to measure the cutting forces along with the amplifier (Kistler 5010), and the LABVIEW 14.0 can be see in Figure 17d.

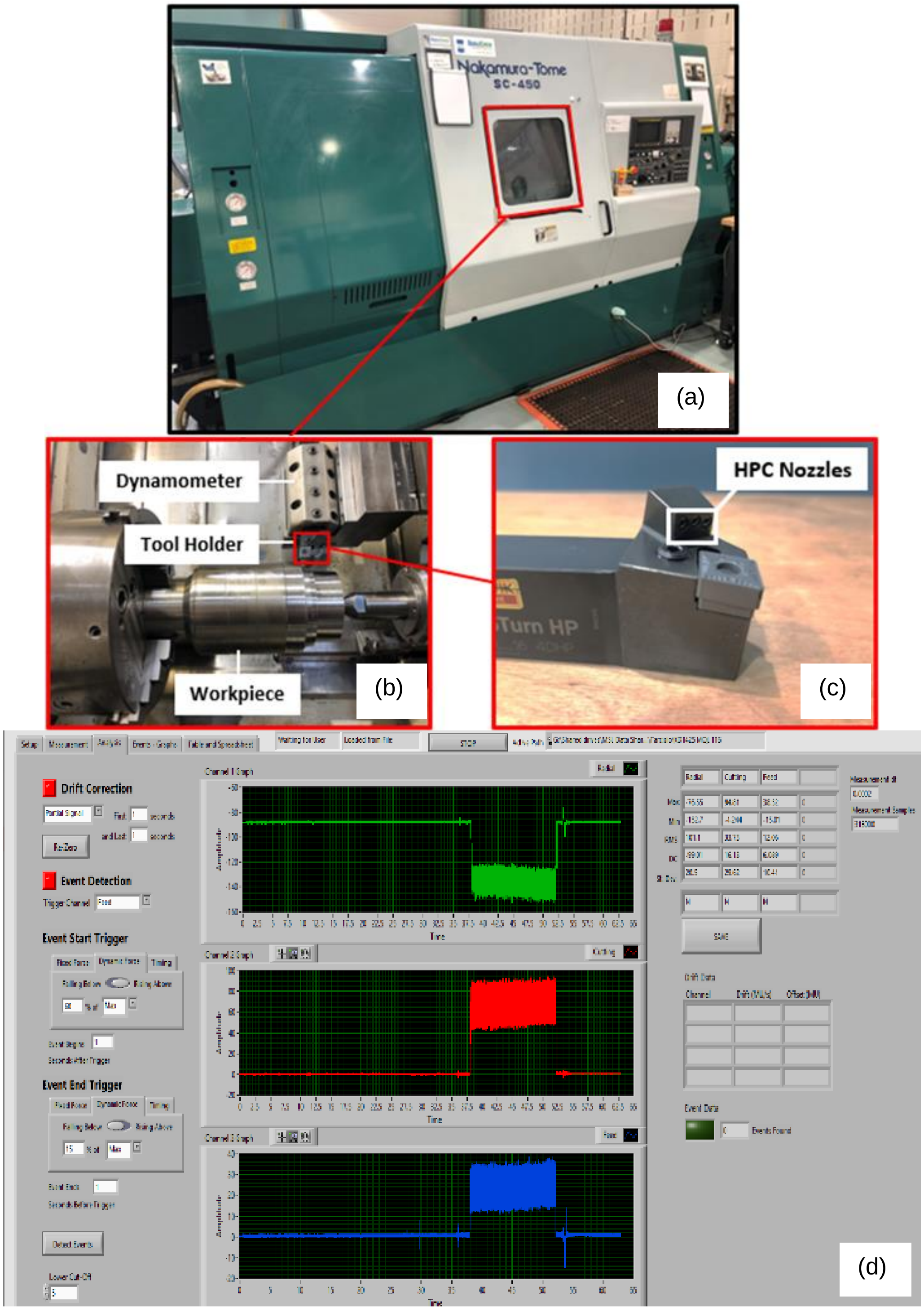

Figure 17: Machine set-up.

- Evaluation of different tool materials - In this step, the tests were divided into three stages. During the stage I, different cut tools materials were evaluated. Eleven different classes of inserts were tested. Tests were stopped when the tool reached the maximum flank wear of 300 microns or 500 meters of cut length, whichever came first. All inserts used in the test are described in Table 8.

On stage 2, based on the cutting conditions tested on the previous stage, the machining parameters were defined. Cutting speeds of 200 m/min, feed rate and depth of cut at 0.1225 mm/rev and 0.25 mm, in the same order. Finally for the subsequent tests with cutting tools under wet conditions, the cutting fluid chosen was a semi-synthetic HOCUT 795 fluid typically at 6% concentration. High cutting speeds were applied to simulate harsh conditions during machining, therefore, accelerating wear mechanisms. The result for this initial stage is presented in Figure 18.

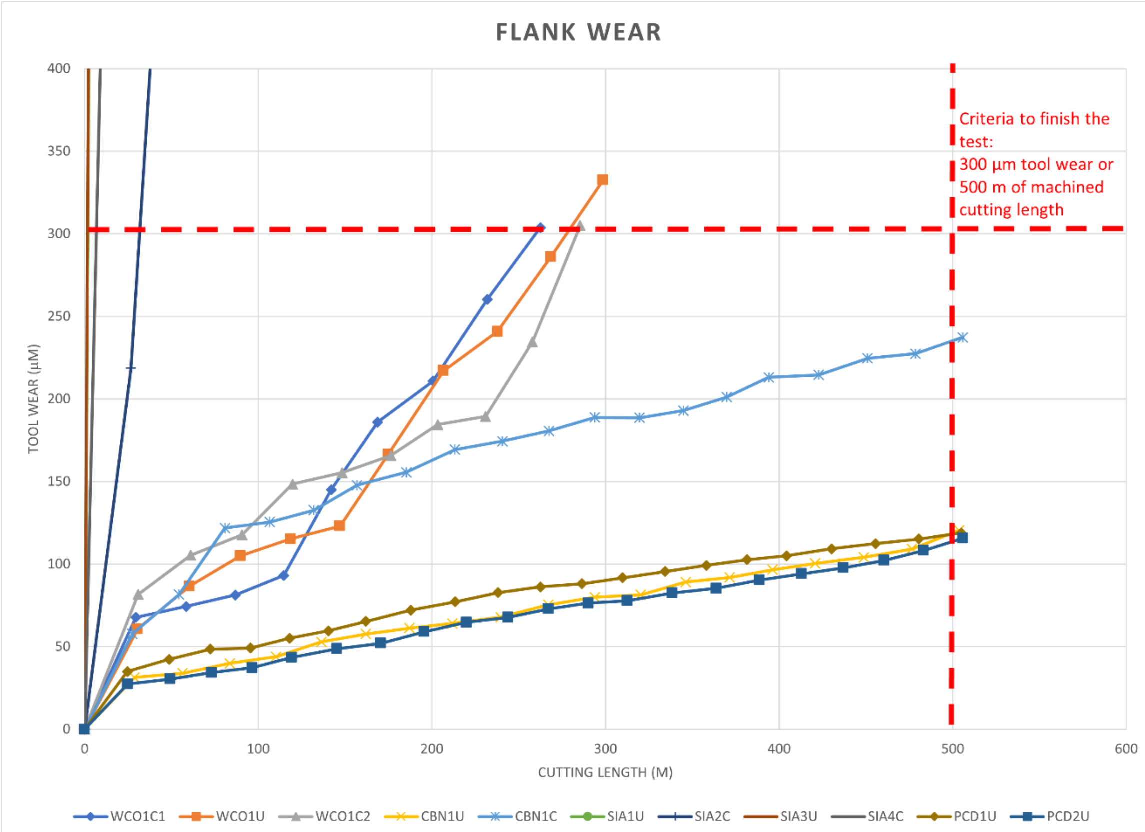

Figure 18: Result of initial stage

According to the results presented on Figure 18, the following cutting tools (PCD1U, PCD2U, CBN1U CBN1C) were selected for the next research step, where different coolant modes were evaluated. The selected tool properties can be seen in Table 9.

Table 9: Tool properties [15]

Tool	**Material**	**Coating**	**Hard phase wt. %**	**Binder**	**Grain size μm**	**Density g/cm³**	**Hardness GPa**	**Modulus GPa**	**TRS MPa**
CBN1U	CBN	-	50	Co/Ni/W/B	2-4	4.3	45	665	-
CBN1C	CBN	PVD AlTiN	50	Co/Ni/W/B	2-4	4.3	45	665	-
PCD2U	PCD	-	15	Co	0.5-1	4.4	> 60	827	2387
PCD1U	PCD	-	11.5	Co	2-30	3.9	> 60	883	1521

- Evaluation of different coolant modes - The four best inserts were returned to the machine to reach the maximum flank wear of 300 microns (according to the ISO 3685). After turning tests with lubricating fluid, the inserts were tested with different coolant modes: dry machining, high pressure coolant, MQL and super absorbent coolant.

In order to evaluate and understand the output parameters, (tool life, wear mechanism, cutting force, friction in the cutting zone, machined workpiece) flank wear measurements were taken after approximately 30 meters of machined cutting length, at each measurements an optical microscopy image of the worn inserts' rake and flank surfaces were taken using an Optical Microscopy Keyence VHX-5000 (Figure 19a). To study the friction in the cutting zone and understand the chip formation process, the chips were collected at the end of the initial cutting step (approximately 30 meters of cut), to evaluate the tribological conditions on the tool chip interface. Alicona Infinite Focus (Figure 19b) optical microscope with white light interferometry for 3D surface measurements of the damaged inserts and collected chips. Also, a Tescan VEGA2 Scanning Electron Microscope (SEM) (Figure 19c) was employed to acquire high magnification images of surface topography of the chips and worn cutting inserts. To evaluate the friction conditions of the cutting process based on surface topography analysis, the chips were collected and evaluated following the procedures described in section 3.3.

Figure 19: (a) Optical microscopy images Keyence VHX-5000, (b) Alicona Infinite Focus, (c) Tescan VEGA2 Scanning Electron Microscope

3.3. Surface integrity

Following the cutting tests, three separate characterizations techniques were performed to investigate surface integrity: surface texture, hardness profile, and residual stress measurement. More details on these characterization techniques will be provided in the next sections.

3.3.1. Surface texture

Following the machining tests, the surfaces created by each tool were sectioned into smaller samples using a waterjet. Each coupon sample was cleaned in an ultrasonic solution with ethanol for 280 seconds prior to undergoing Alicona analyses. In these analyses, the surface texture was computed by the built-in surface texture module, using the 100x lenses to scan a randomly sampled 1 mm^2 region of each machined surface.

3.3.2. Cross section hardness profile

Another collection of coupon sample was placed in epoxy resin and metallographically prepared using standard methods until a mirror-polished surface was achieved, followed by etching with the same reagent stated in item 3.1. Following etching, the samples were subjected to microhardness testing on a

Nano-Indenter hardness tester equipped with a Berkovich indenter. Loads of 50 mN were applied for a period of 10 seconds. The matrix contained 15 points divided into five lines and three columns, with measurements beginning at 5 microns from the machined surface and a spacing of 10 microns between each indentation.

3.3.3. Residual stresses

Residual stresses on the machined surfaces were calculated using the X-ray diffractometry process on an LXRD diffractometer with Cu radiation. The scans were carried out at 25kV and 30mA. The 213 planes with a Bragg angle (2θ) of 142 degrees with an oscillation of (β) 3 degrees was selected to be investigated. Figure 20 shows a total of 20 measurements taken for each sample perpendicular to the cut. For this analysis, the best tool life came from the PCD1U tool which was selected tested under the following conditions (Flood Worn and New, HPC Worn and New and MQL Worn and New).

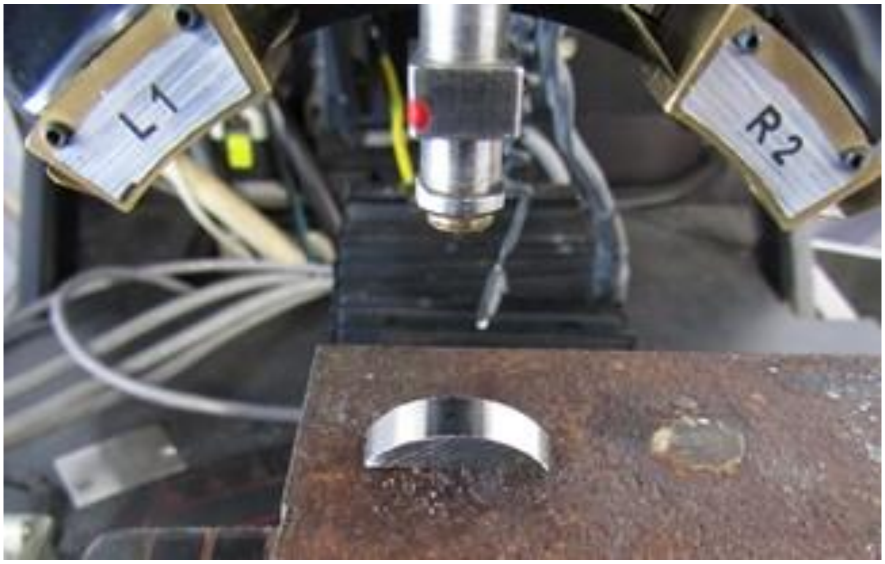

Figure 20: Setup parameters to measure residual stress.

4. Results and Discussion

In this chapter, the results will be organized according to the flowchart of the experimental methodology shown in Figure 16 on the previous chapter. Starting with the analysis of the results of the machining tests and then with the characterization of the work materials, which will be discussed based on images and comparative charts. Regarding the performance of the cutting tools tested under different coolant conditions, the obtained results will also be discussed and evaluated based on the tribological conditions for each coolant mode tested.

4.1. Tool life and wear studies under different coolant modes

To identify the wear mechanisms and find the best tool substrates four different tool materials (Table 9) were tested during machining of Ti5553 under dry, flood coolant, High-pressure coolant (HPC), minimum quantity lubrication (MQL) and Super-Absorbent Coolant (SAC) conditions. The initial cutting tests were performed under the selected cutting conditions explained on section 3.2 from the Experimental procedures – cutting tests (cutting speed 200m/min, feed rate 0.1225 mm/rev, and depth of cut 0.25 mm). The goal of this section was to identify the best substrate material under the different coolant modes under longitudinal turning tests during the machining of Ti5553. The results of cutting tool wear are shown in Figure 21.

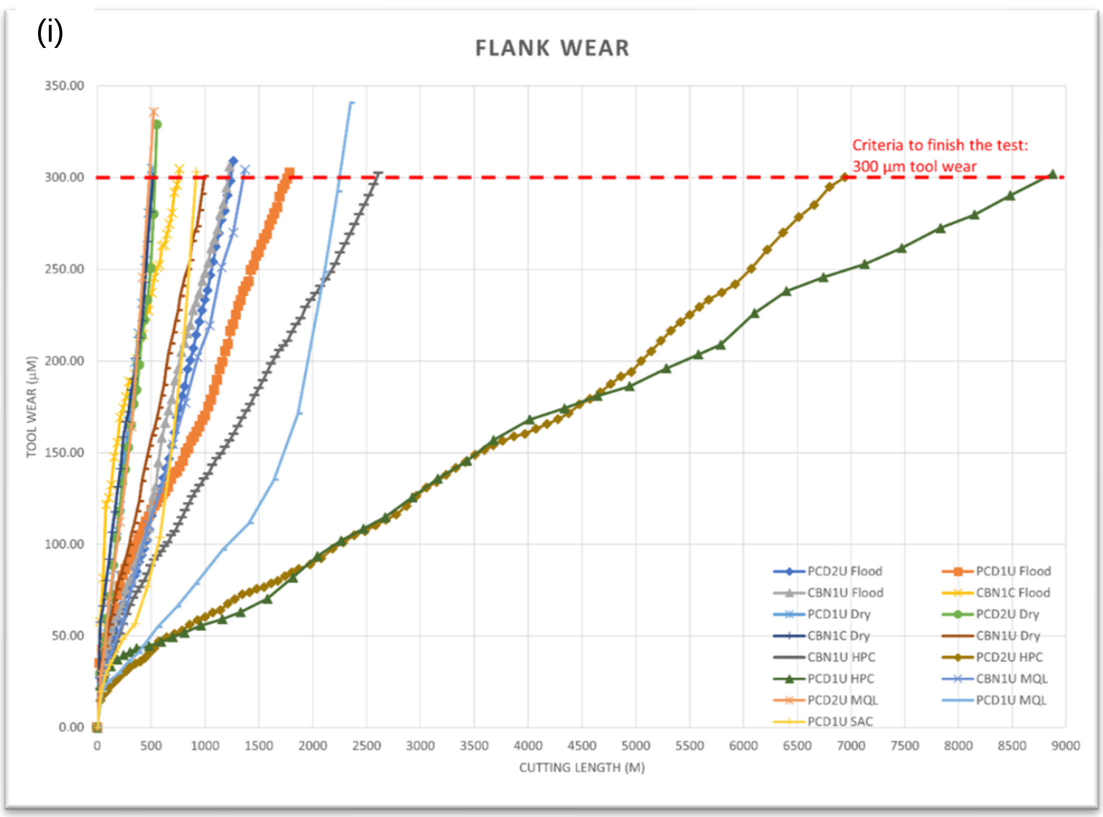

(ii)

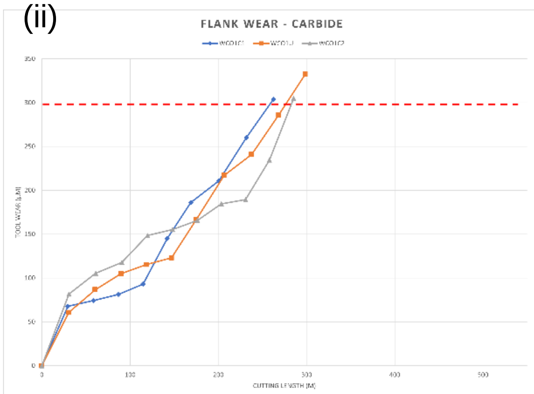

a) Carbide

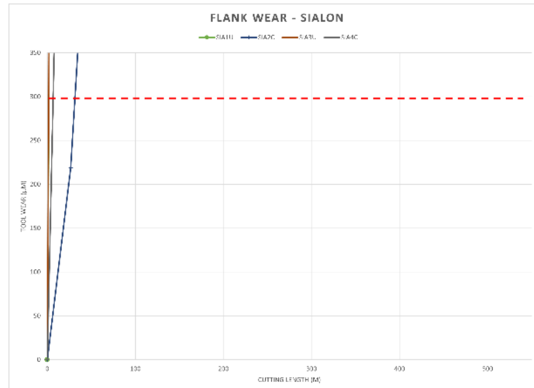

b) SiAlON

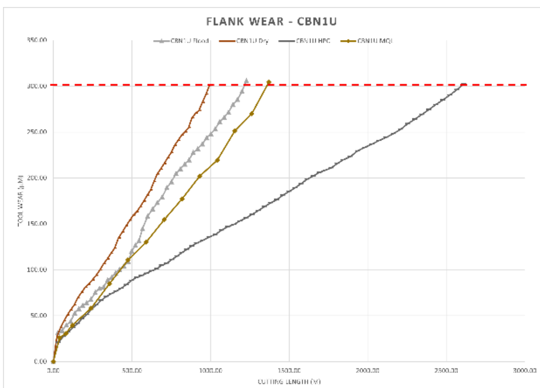

c) CBN1U

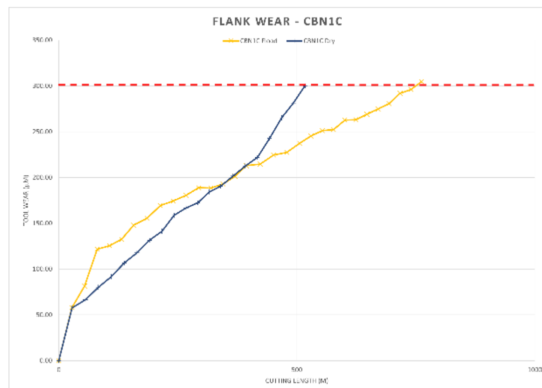

d) CBN1C

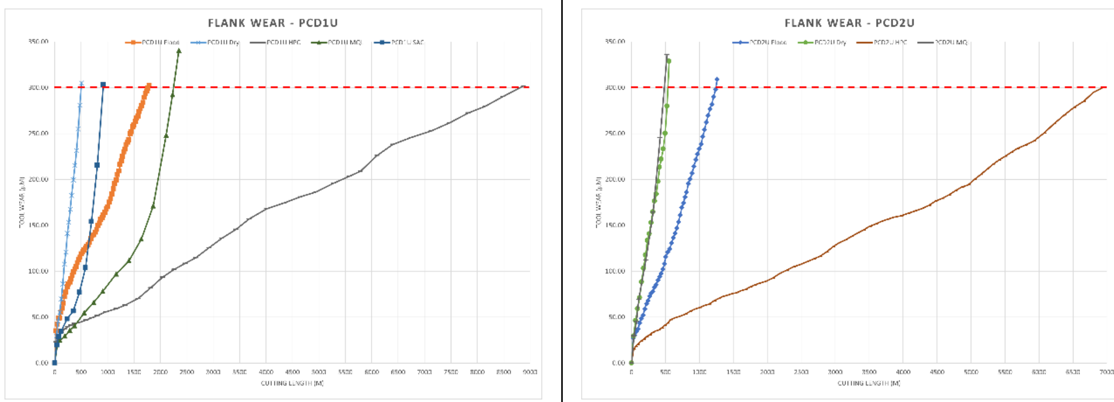

e) PCD1U

f) PCD2U

Figure 21: (i) Tool wear in Flood, Dry, HPC, MQL and SAC; (ii) tool wear for different tools separated.

According to Figure 21, the maximum flank wear adopted is VB (0.3 mm) for each cutting insert tested in this work. The findings indicate that the process of tool wear is strongly dependent on the coolant conditions. As shown in Figure 21, only three combinations of cutting tool materials and coolant modes (CBN1C Dry, PCD2U HPC and PCD1 HPC) were capable of exceed 2500 m of cutting length without surpassing the end-of-life requirement (300 µm flank wear). Under a HPC mode the PCD cutting tools had improved wear resistance, while under Dry conditions CBN1C performed better compared to the other tools and conditions.

Figure 22 illustrates the tool life in minutes. CBN1C shows low performance under flood and dry conditions. The criteria considered to evaluate the tool performance was 5 min of cutting time on either dry or flood conditions. The CBN1C did not reach these criteria and for this reason this tool material is not considered for the other coolant modes. Once the HPC coolant mode is applied the tool life increases substantially. The best tool life is achieved by the cutting tool PCD1U with a cutting time of 45 min approximately.

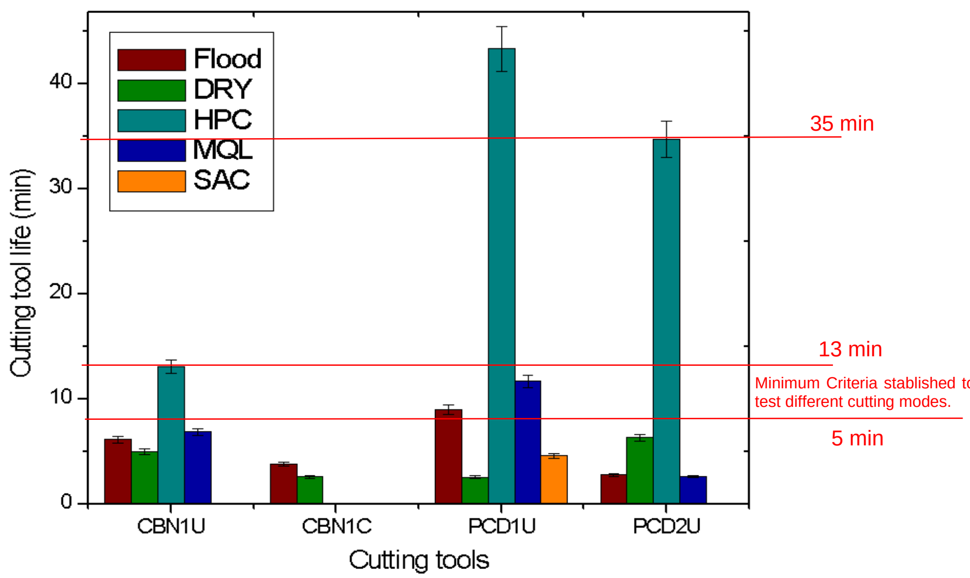

Figure 22: Lifetime for each tool

At any of the coolant modes tested, the PCD1U cutting tool showed better tool performance than the other tool materials tested. It is recommended that the cutting speed and cutting tool combination be balanced to improve efficiency while also extending tool life. Arrazola et al., [9] explains that the initial conditions to perform the cutting and the tool material could significantly affect the performance of the cutting tool and the wear mechanisms during machining of Ti5553.

In order to have a uniform wear comparison, the Table 10 represent the tool wear images, based on intervals defined in Figure 22.

Table 10: Tool wear images

Tool Life	Tool and coolant modes		
	CBN1U	PCD1U	PCD2U
5 min	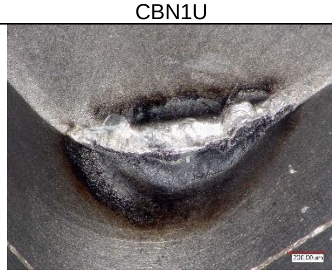 Flood	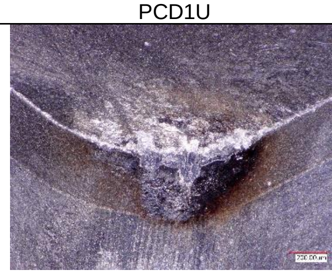 Flood	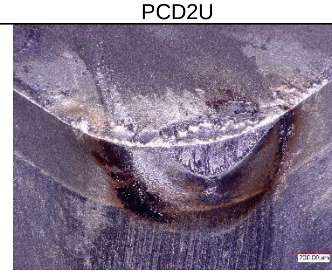 Flood
	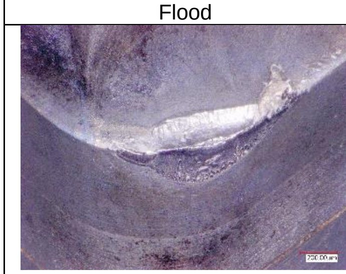 Dry	Test not completed. Early tool Failure	Test not completed. Early tool Failure
	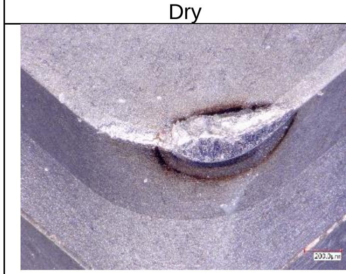 HPC	 HPC	 HPC

	 MQL	 MQL	Test not completed. Early tool Failure
13 min	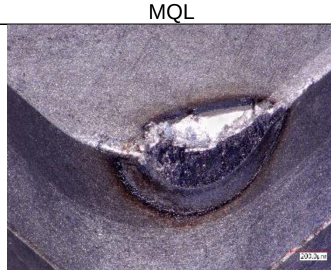 HPC	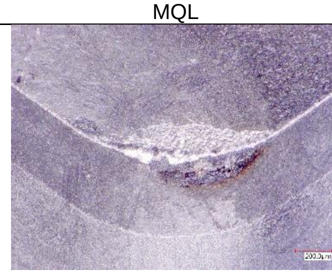 HPC	 HPC
35 min	Test not completed. Early tool Failure	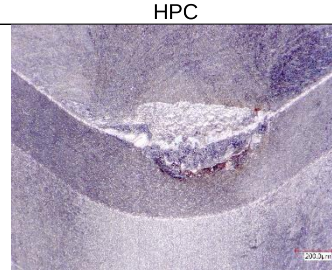 HPC	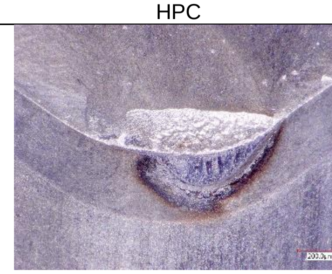 HPC

To understand the wear mechanisms under different coolants the following section will explore and provide more details about the wear behavior of the four different substrates tested during this work.

4.2. Wear mechanisms studies

To understand the wear behavior of the cutting tools, SEM analyses were performed on the inserts after the machining tests. The SEM images of the worn tools can be seen in Figure 23. The results contrast the tool wear morphology obtained for each cutting tool tested based on the cutting test results (Figure 21) at the end of the tool life. These studies include a thorough investigation of the tool wear trends that occur during cutting. The results show a poor performance of the CBN1U and CBN1C cutting tools during machining. This fact can be explained by the high temperature generated in the region of the cut and, since this is the machining process of a material with low thermal conductivity, this generated heat is transferred intensively to the tool, thus resulting in the combination of different wear mechanisms. For all coolant modes, adhesion is the most common wear mechanism seen in both sets of tools tested. This wear mechanism is also accompanied by oxidation and abrasion wear (Figure 23). Typically, machining of Ti5553 is distinguished by extensive work hardening and high cutting temperatures [17].

Coolant	CBN1U	CBN1C
Flood	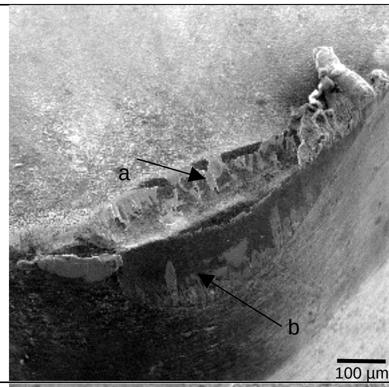	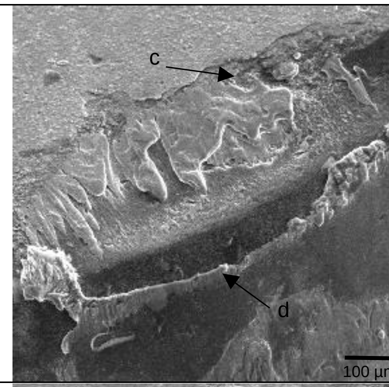
Dry	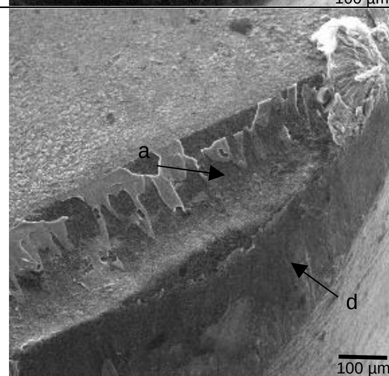	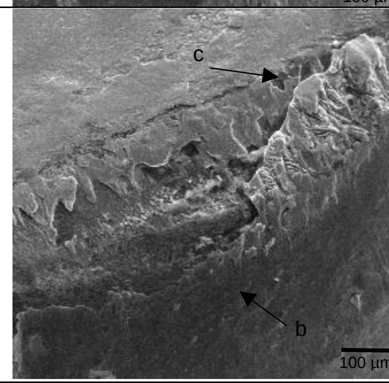
HPC	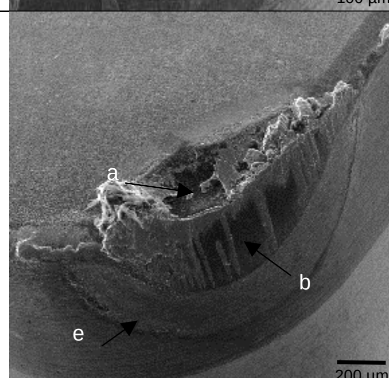	Test not completed. Early tool Failure
MQL	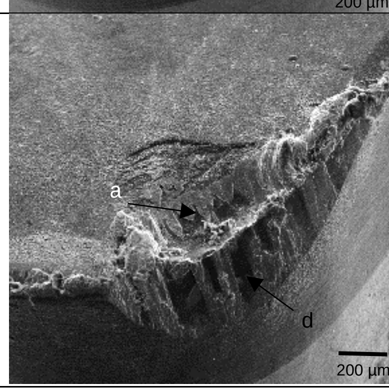	Test not completed. Early tool Failure

Coolant	PCD1U	PCD2U
Flood	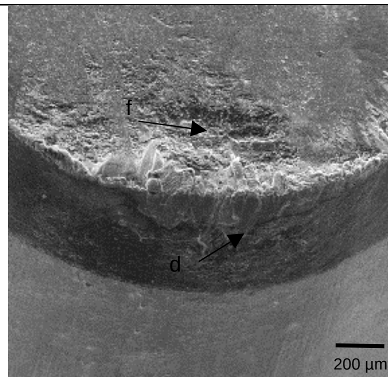	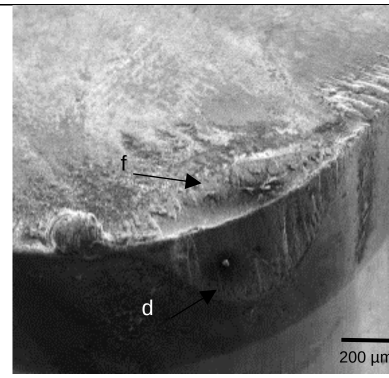
Dry	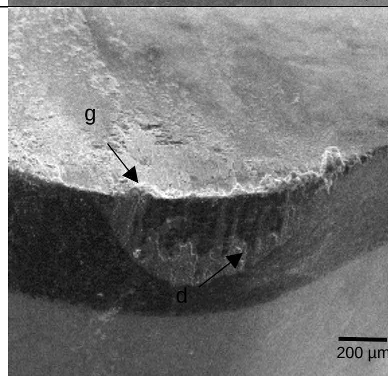	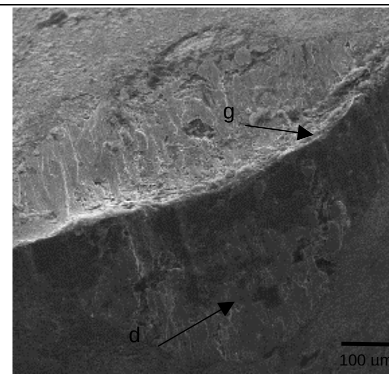
HPC	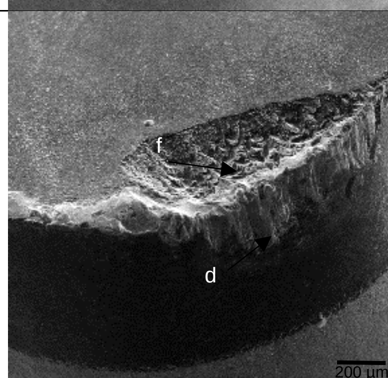	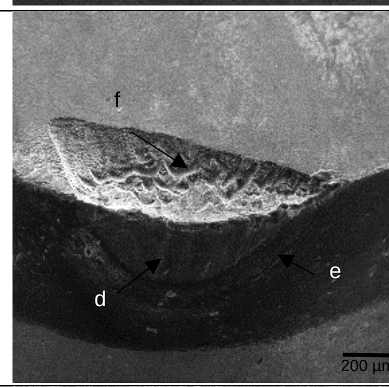
MQL	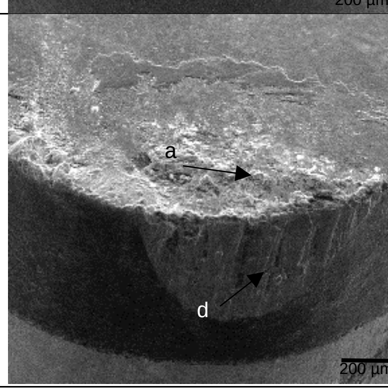	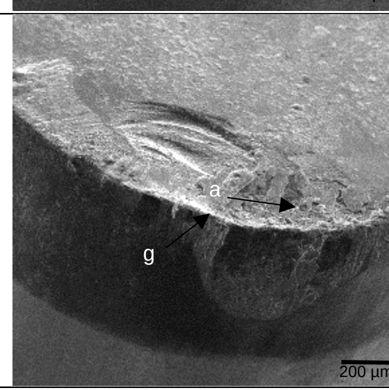

SAC	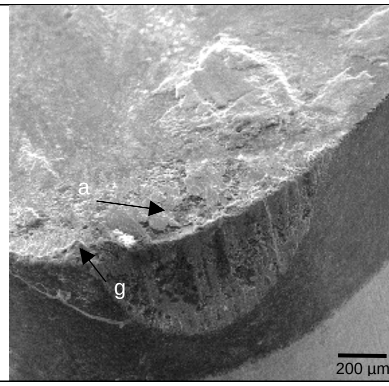	Test not completed. Early tool Failure
	a. Crater wear covered by BUE b. Abrasion c. Substract exposure d. Combined effect of Adhesion and Abrasion marks e. Oxidation f. Crater wear g. BUE	

Figure 23: SEM Analyses (worn tools stage, end of the life)

This combination of wear mechanism should result in an unpredictable friction wear mode that usually produces an extreme build-up-edge formed by adhesive bonds at the tool`s rake face and the workpiece material interface (BUE). Furthermore, the cutting tool cannot withstand high loads when cutting, flaking off the cutting tool material. This avalanche effect produces chipping, substrate exposure, and catastrophic tool failure. This effect is reduced for the PCD cutting tools specially under flood and HPC coolant modes (Figure 23). Under HPC, the SEM images also demonstrate that the geometry of crater wear is roughly twice as that observed for the same tools under flood conditions. This is clear evidence of long tool life (near to 9000 m against near 2000 m in flood condition) which is supported by the presence of HPC that reduces the contact area between the chip and the cutting tool, improving the sliding conditions within the cutting zone. According to this approach, these cutting tools under this condition show friction reduction at the chip/tool interface. As a result, only abrasion and oxidation can be seen as the major wear mechanism.

Additionally, volumetric tool wear measurements revealed the surface peaks and valleys produced on the cutting tools during the machining tests. These data were obtained at the end of the tool life. The 3D tool wear analyses are shown on Figure 24.

Coolant	CBN1U	CBN1C
Flood	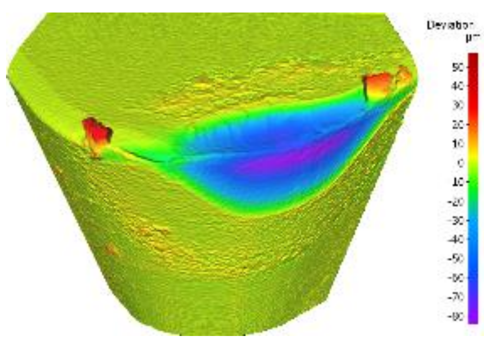	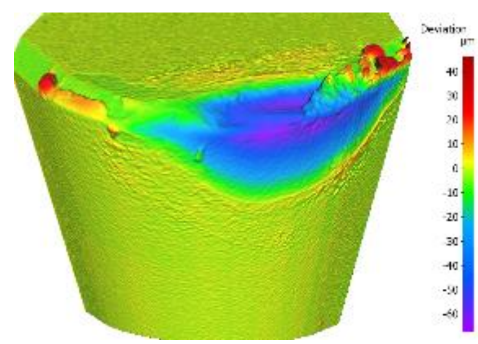
Dry	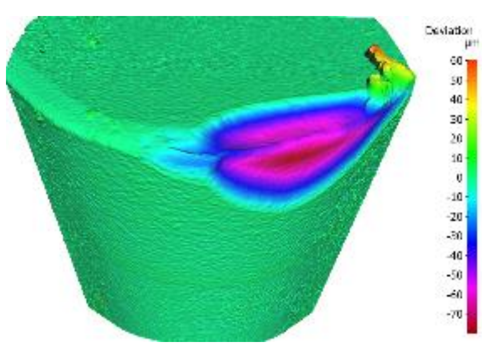	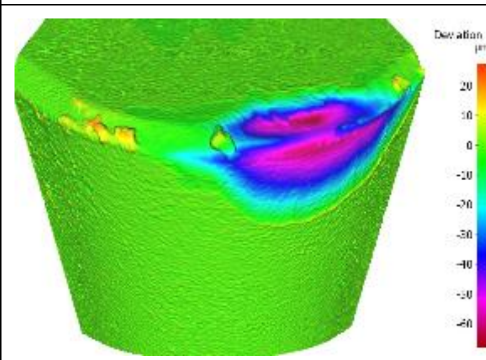

<table>
<tr><td>HPC</td><td>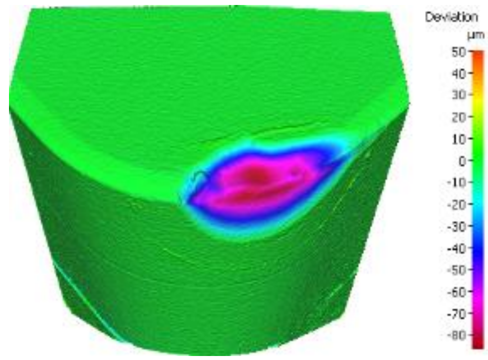
</td><td>Test not completed.
Early tool Failure</td></tr>
<tr><td>MQL</td><td>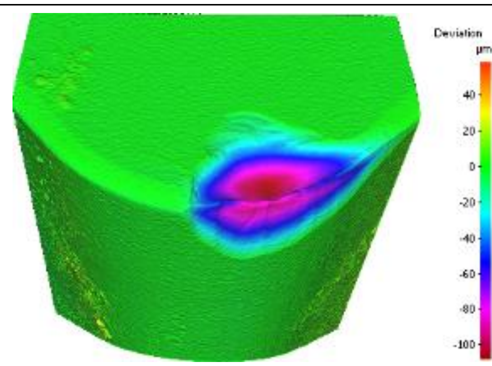
</td><td>Test not completed.
Early tool Failure</td></tr>
<tr><td>Coolant</td><td>PCD1U</td><td>PCD2U</td></tr>
<tr><td>Flood</td><td>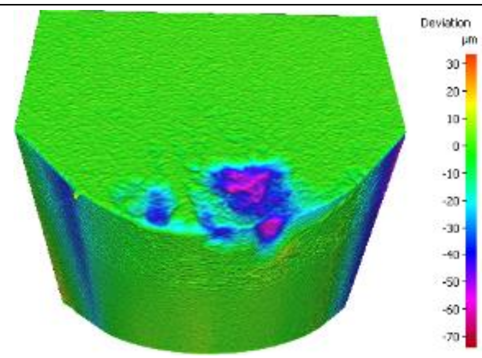
</td><td>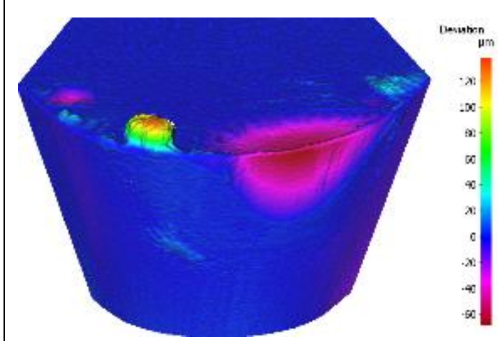
</td></tr>
<tr><td>Dry</td><td>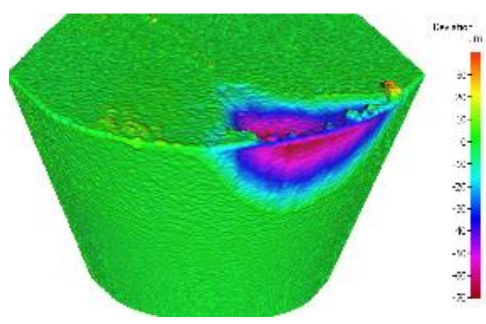</td><td>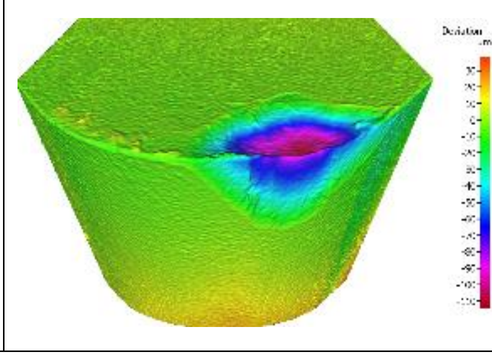</td></tr>
</table>

HPC	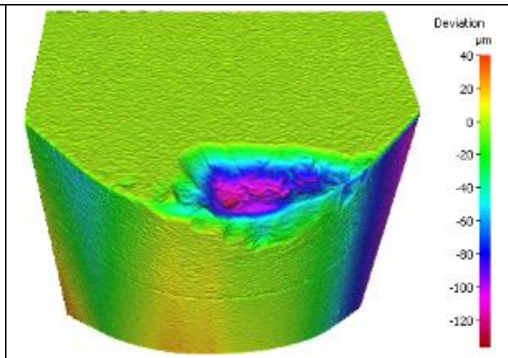	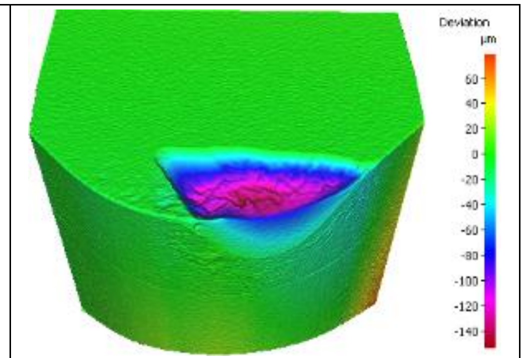
MQL	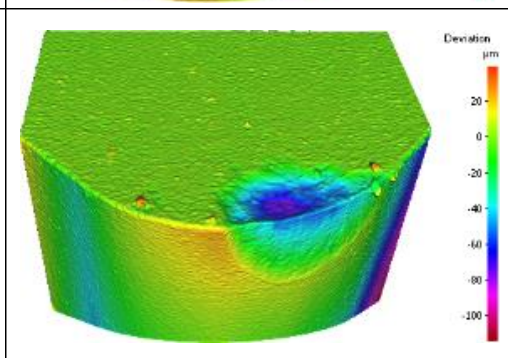	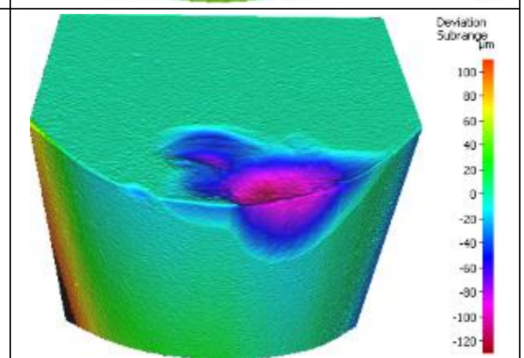
SAC	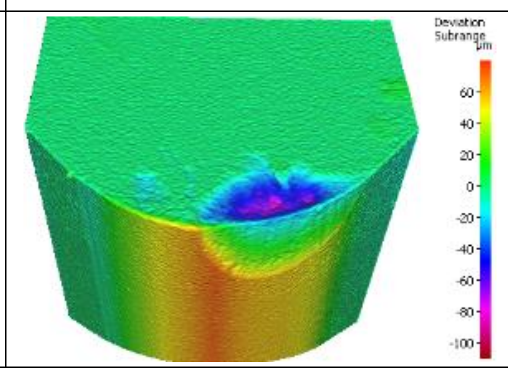	Test not completed. Early tool Failure

Figure 24: 3D tool wear analyses (worn tools stage, end of the life)

For the CBN tools under all coolant modes, a considerable crater wear could be found for both CBN grades (1U and 1C). This indicates that those cutting tool materials cannot sustain high temperatures and heavy loads which are the minimum requirements to be considered when machining the Ti5553 alloy. A slight amount of build-up edge (BUE) was observed on the CBN tools under dry and flood conditions. On the other hand, under the HPC condition the crater wear on the rake surface of the PCD cutting tools was greater than that of the CBN tools. That can be explained by the long tool life produced by these cutting tools in comparison with the CBN ones (approximately 300 % improvement), still, this performance is a response to the mechanical properties of the cutting tool. As presented in Table 9 this tool material shows superior hardness and elastic modulus as well as high chemical stability, which is critically essential to machining the Ti5553. This characteristic reflects in less oxidation wear and improve the tool performance at high cutting speeds. The opposite behaviour could be detected for CBN cutting tools.

As it is well known, the BUE generated during the cutting is an unpredictable mechanism that causes cracks, chipping, and substrate exposure, all of which can lead to catastrophic failure. However, this effect is clearly minimized for the PCD grade tools [7].

According to the results obtained from the investigation carried out on SEM and Alicona, it is possible to affirm that the wear mechanism found three different pathways as the major contributors, those are: Chemical affinity between the tooling material and the workpiece; cutting zone contact area which is directly affected by the coolant mode, and the combination of high temperature and heavy loads typically found during machining of the Ti5553 alloy. Therefore, the HPC coolant mode promotes a better reduction on the cutting zone contact area (interaction between the chip and the tool's rake face), thus reducing the interaction period of both materials, reducing the cutting loads and heat in the cutting zone in response to this effect. Finally, the combination of those events reduces the oxidation action which might lead to increased tool life. To understand these aspects, the next section will discuss the tribological aspects in the cutting zone for the following cutting tools (PCD1U, PCD2U and CBN1U) under the coolant modes (HPC, MQL and SAC).

4.3. Tribological aspects of the cutting

Usually when machining aerospace alloys with very low depth of cut, its expected that the forces acting at the tool and the workpiece can be reduced at high cutting speed - primarily because the high temperatures reduce the strength of the work material [4]. The cutting forces produced are combined responses of the tribological interaction of both materials as well as the cutting conditions (cutting parameters and lubrication) developed in the cutting zone [9]. To evaluate the tribological cutting scenario the cutting forces were collected at the beginning of the cut for the selected tools and conditions. The results are presented in Figure 25.

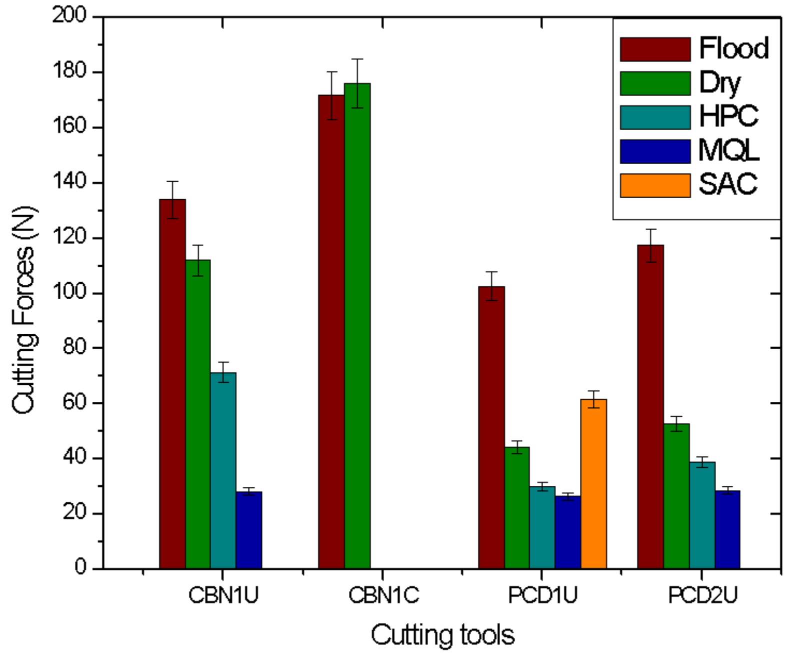

Figure 25: Cutting forces in the first pass.

Interestingly, most of the cutting forces collected during the experimental studies showed that application of MQL reduces the cutting forces. This signifies that this coolant mode can improve the friction coefficient in comparison to the other coolant methods. Although this method cannot sustain this positive effect for a long time, this can be a good solution to machining Ti 5553 rather than Dry or flood modes (Figure 21). As confirmed by Figure 22, this method produced superior tool life in relation to these two methods. On the other hand, when machining low thermal conductivity material like Ti, high temperatures are found in the cutting zone, thus this method cannot provide enough cooling to reduce the heat. Consequently, oxidation wear is accelerated over time and tool life is reduced [16]. This explains the inferior tool life under MQL in comparison with the HPC mode (Figure 21).

In combination with the cutting forces, chips produced during the initial stage of the cutting were collected and considered as subject of studies to support the understanding of the tribological aspects of the cutting process for each condition tested. Chip’s geometry and morphology in machining are determined by the combined effects of the material properties, the cutting parameters, and the tribological interaction between the tool’s material and the workpiece [7]. To understanding the chip formation process, Figure 26 contains the images of chips collected at the initial stage of the cutting for each coolant mode tested.

Coolant	**CBN1U**	**CBN1C**
Flood	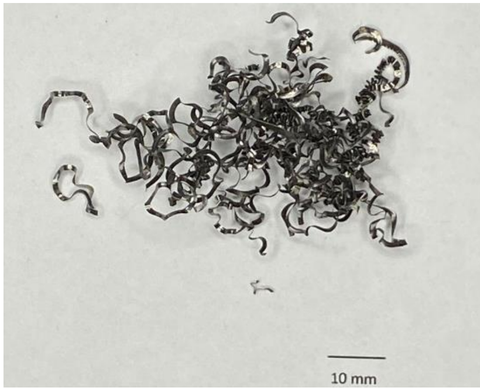 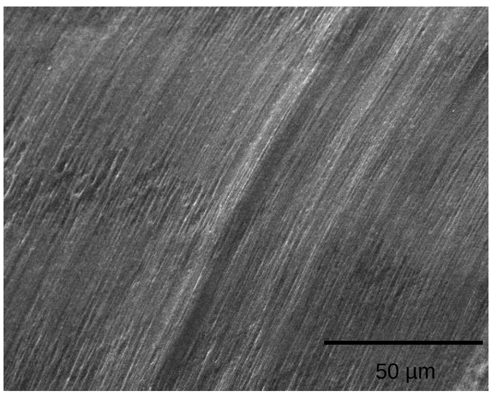	 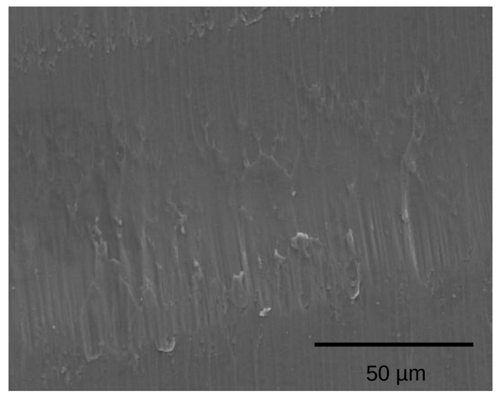
Dry		

	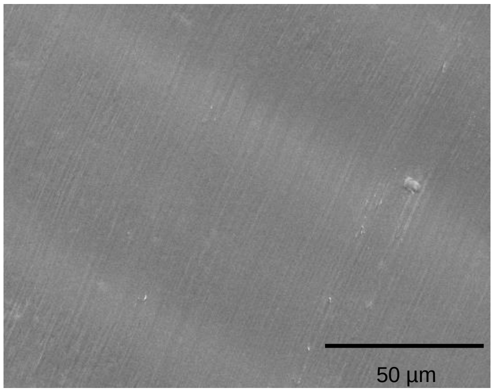	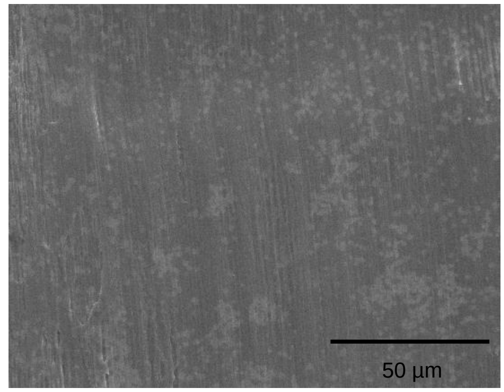
HPC	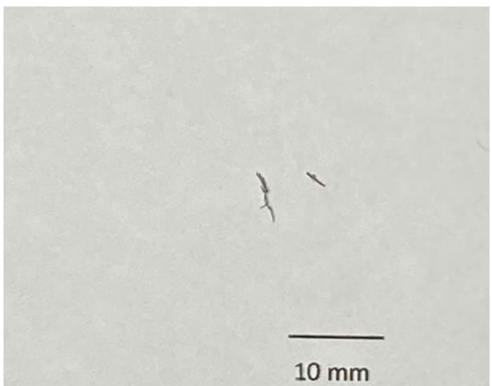 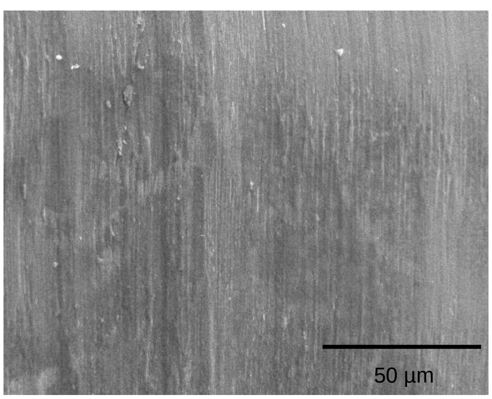	Test not completed.

<table>
<tr><td>MQL</td><td>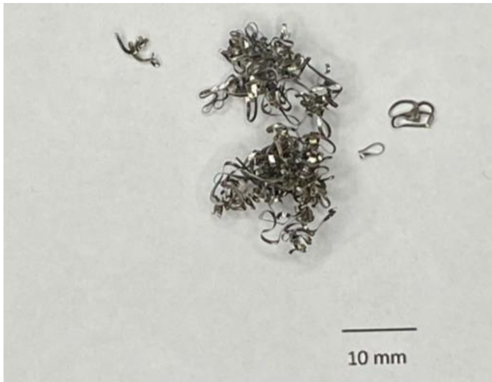

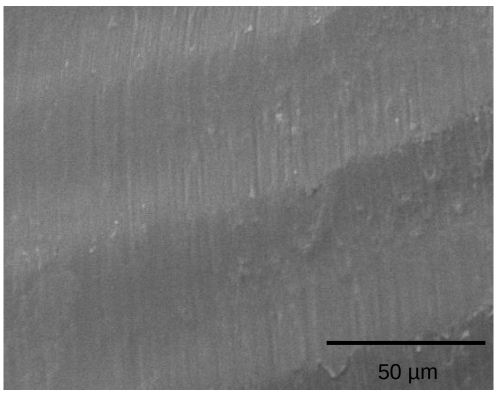
</td><td>Test not completed.</td></tr>
<tr><td></td><td>PCD1U</td><td>PCD2U</td></tr>
<tr><td>Flood</td><td>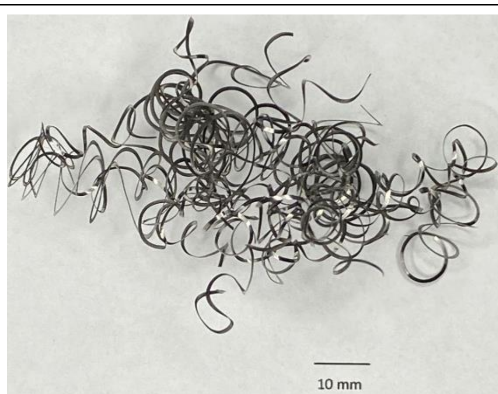
</td><td>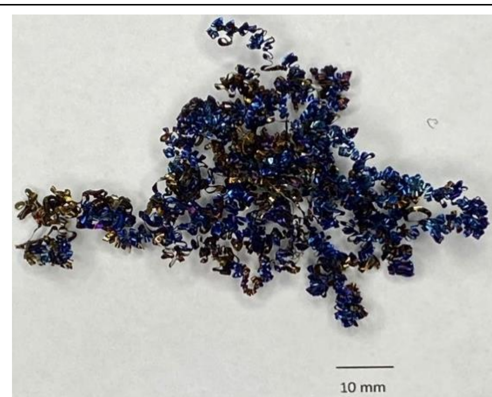
</td></tr>
</table>

	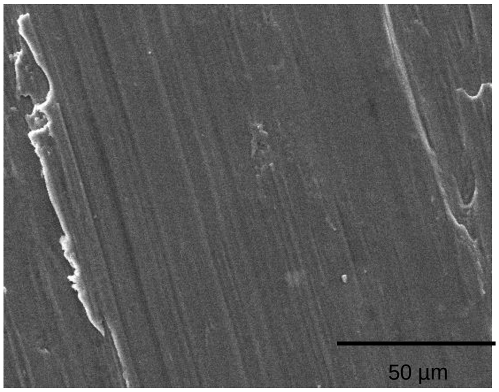	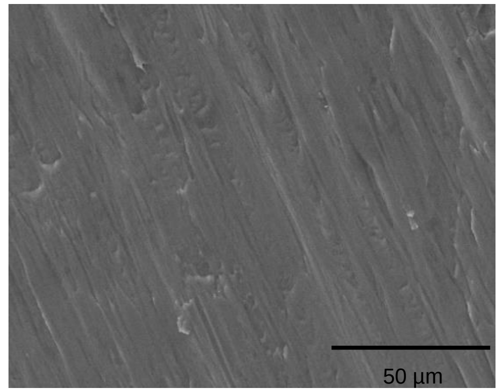
Dry	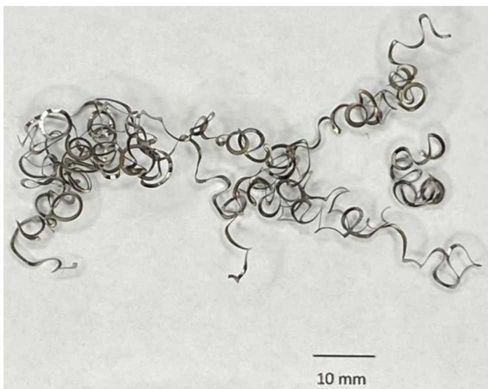 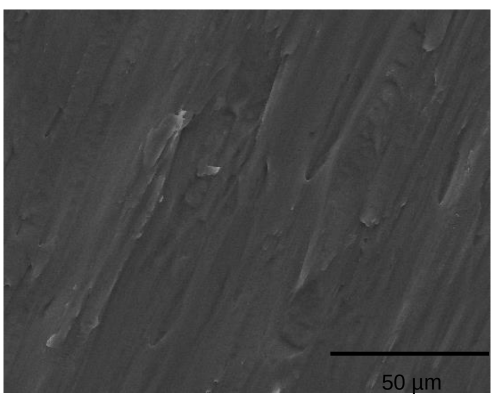	 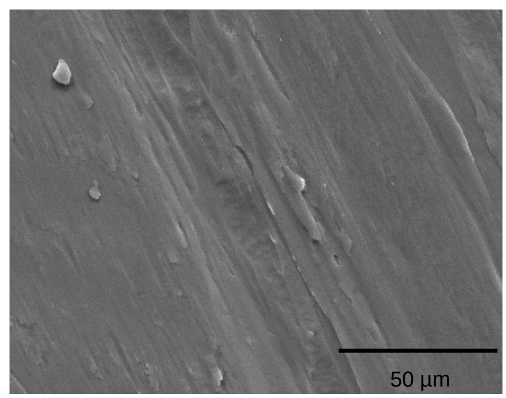

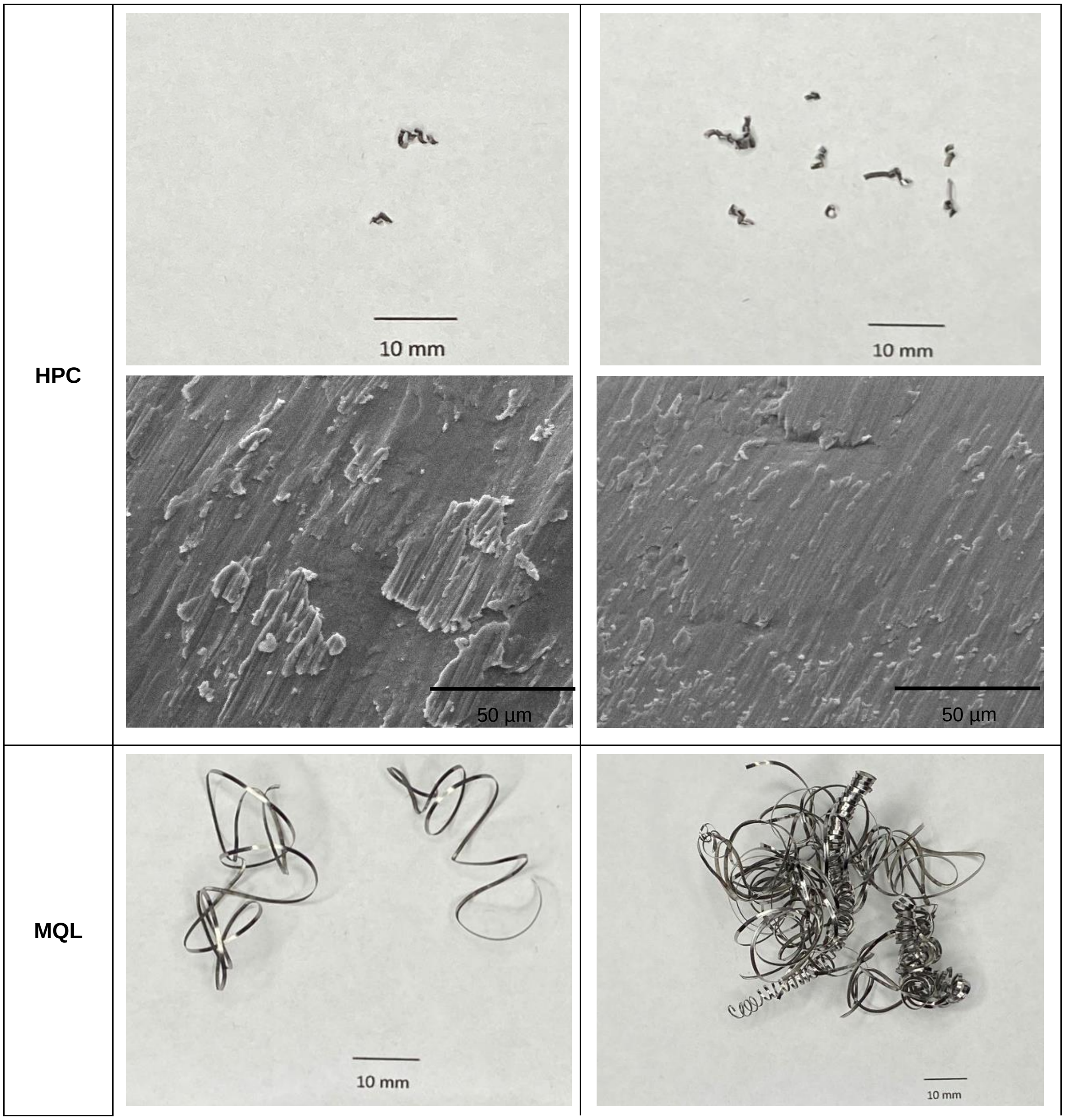
HPC
10 mm
10 mm
50 µm
50 µm
MQL
10 mm
10 mm

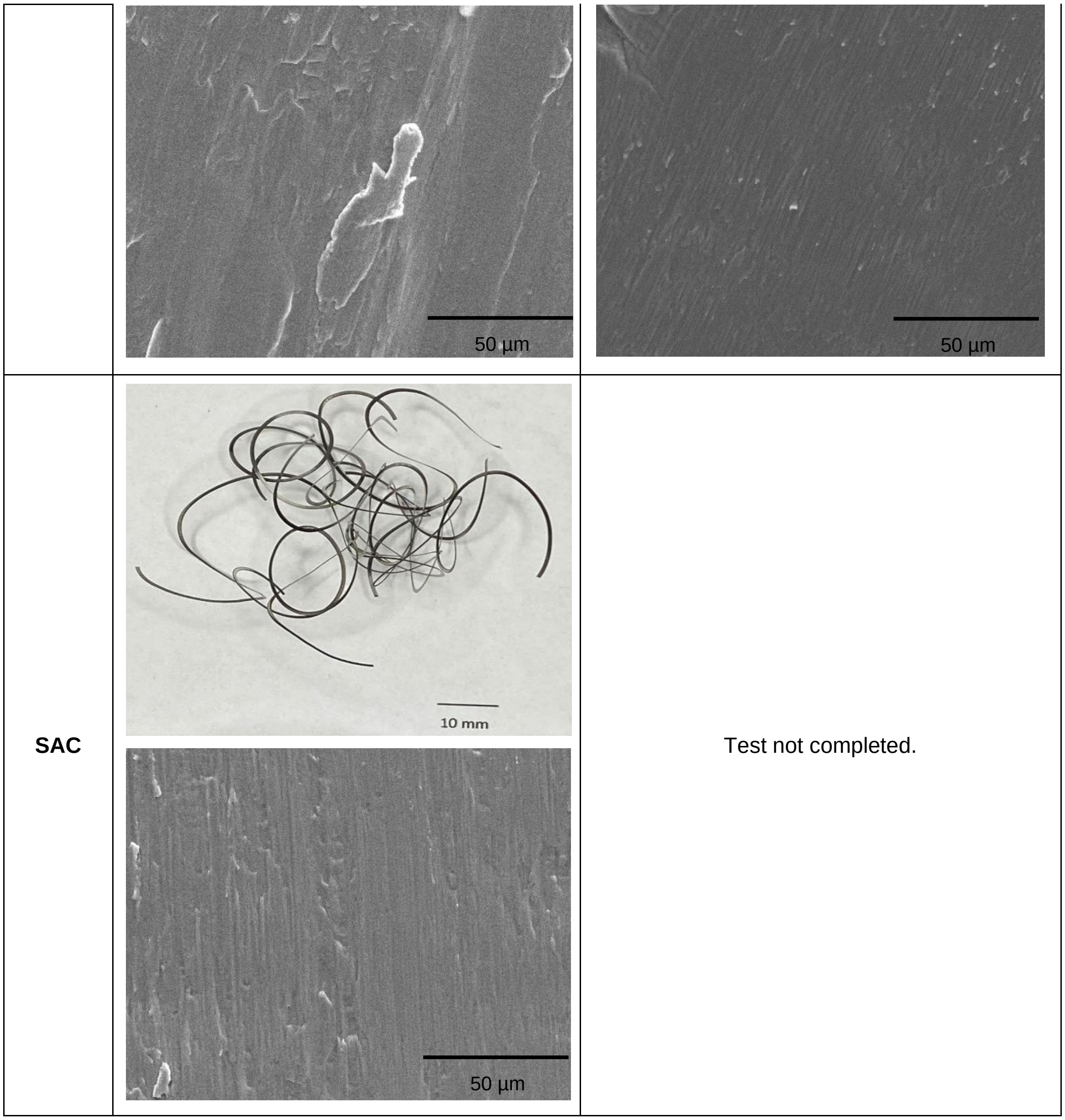

Figure 26: Chips collected at the initial stage.

Usually, the type of chip and the morphology of the bottom surface of the chip are direct indicators of friction conditions at the tool / chip interface. By studying the optical images of the chip's geometry, the impact of HPC on chip characteristics is noticeable. Under HPC mode, the chips obtained are shorter in comparison with those obtained under the other coolant methods studied in this thesis. These characteristics are clear evidence that the HPC contributes to breaking the chip immediately when the chip is formed. Under HPC method, the SEM obtained on the chip undersurface suggests that the chip breaks out from the sticking zone without having a displacement through the sliding zone. This effect totally changes the chip formation process and as a result, HPC minimizes the tool/chip contact length (TCCL) over the rake face of the cutting tool, thus decreasing the action of mechanical loads acting on that area [7]. As shown by Table 11, the chip sliding velocity, friction coefficient, chip flow angle and tool chip contact length confirm that MQL when applied reduced TCCL and high chip flow lower chip flow angle are obtained. These are an indication that the chip flow during the cutting is essentially generated by seizure on the sticky tool surface. A longer TCCL was detected under flood and dry coolant modes.

Table 11: Tribological conditions of the cut (error ±3%).

Cutting tool	Chip sliding velocity (m/min)				Friction Coefficient (μ)			
	Flood	**Dry**	**HPC**	**MQL**	**Flood**	**Dry**	**HPC**	**MQL**
CBN1U	149.52	165.34	16.95	192.53	0.39	0.36	0.93	0.14
CBN1C	149.56	169.23	N.A.	N.A.	0.41	0.42	N.A.	N.A.
PCD1U	165.30	166.29	15.32	194.68	0.31	0.25	0.87	0.09
PCD2U	162.34	166.98	13.69	192.09	0.33	0.25	0.99	0.12

Cutting tool	Chip flow angle (degrees)				TCCL (mm)			
	Flood	Dry	HPC	MQL	Flood	Dry	HPC	MQL
CBN1U	23.56	23.47	13.49	35.84	0.82	0.63	0.26	0.48
CBN1C	25.35	25.35	N.A.	N.A.	0.84	0.70	N.A.	N.A.
PCD1U	20.09	19.08	12.28	38.26	0.73	0.58	0.22	0.31
PCD2U	20.42	19.10	12.87	36.57	0.77	0.60	0.23	0.33

Overall, the results presented in Table 11 confirms that the effect of MQL as a coolant mode results in better tribological conditions for cutting. TCCL, Friction coefficient and chip sliding velocity confirm this condition for all cutting tools tested. The SAC cutting modes are not tested in this case, due to the lower tool life achieved during the tests.

The PCD1U under MQL coolant mode was the configuration that provided the best tribological cutting conditions. As a result, this combination reduced friction and provided better tool life in comparison to flood and dry modes. This indicates it is a good alternative to be applied to industrial processes.

4.4. Aspects of the surface integrity produced after machining.

To assess the impact of plastic deformation and workpiece hardening produced during cutting operations on the machined surface, Residual stress studies and cross section hardness measurements were performed. Considering the results obtained during the machining tests, only the PCD1U was selected for this study. To evaluate the effect of the coolant mode as well as the tool wear state on the results, Machined workpiece samples were collected based on worn and unworn tools tested under Flood, HPC and MQL modes.

As the result of the plastic deformation induced during machining, a significant difference was found, in terms of surface hardness on the surface and sub-surface layers of the machined part with the use of different coolant modes. Surface microhardness measurements were performed along the cross section. The results are shown in Figure 27.

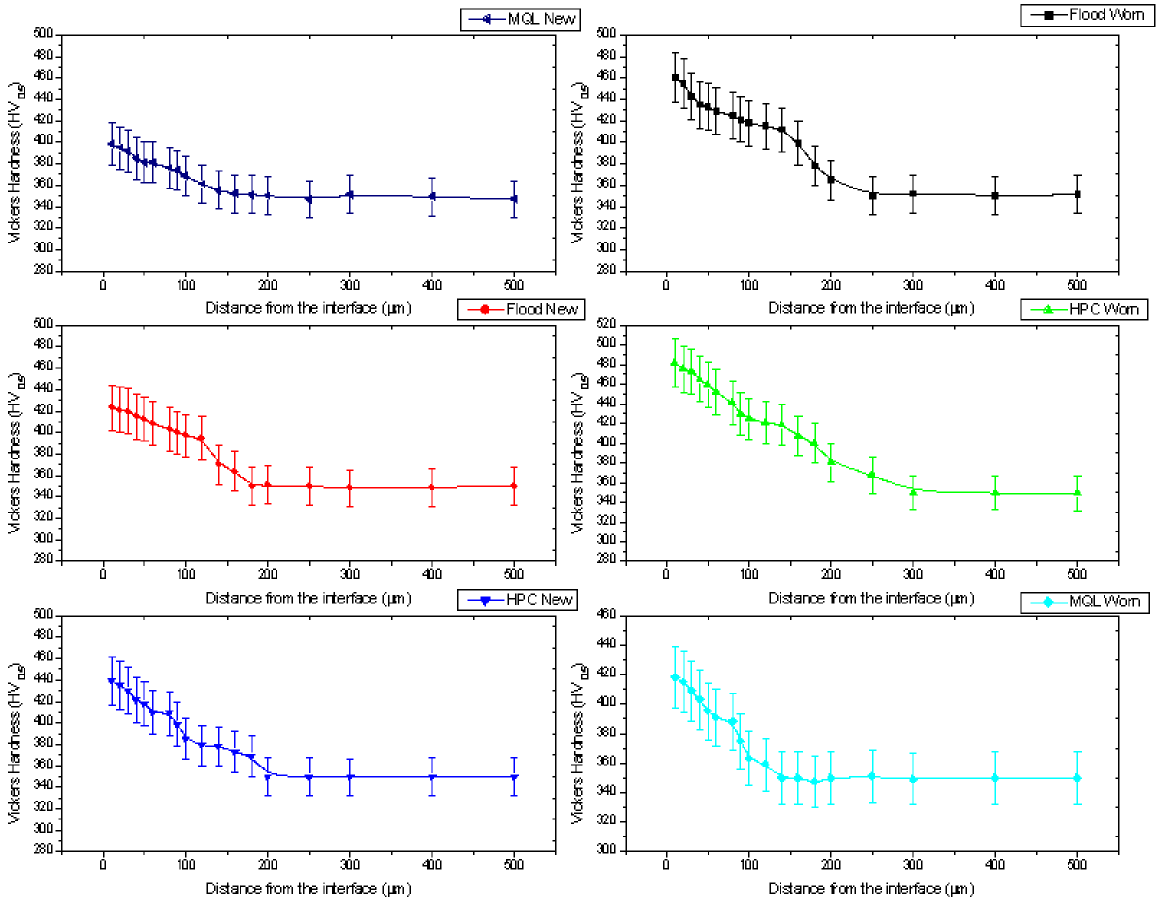

Figure 27: Surface microhardness measurements.

Clearly the results show that under the MQL coolant mode, the effect of work hardening is reduced. To confirm these results, residual stress data was also collected for those samples. Results are provided in Table 12.

Table 12: Residual stress data

Sample	Axial Residual Stress (MPa)
Flood worn	-213 ± 14
Flood new	-262 ± 14
HPC worn	-386 ± 21
HPC new	-207 ± 14
MQL new	-269 ± 12
MQL worn	-7 ± 28

The results indicate lower compressive stress for the MQL, while the surface obtained by machining under Flood and HPC show surface hardening (Figure 27) and high residual stress on the surface of the part machined with MQL. These are effects of hardening that occurs due to the high rate of plastic deformation. In contrast, the application of MQL to the improvement of friction conditions. This resulted in a better surface finish and, consequently, reduced the hardening effect on the surface, as well as the microstructural damage to the part.

5. Conclusions

The research conducted in this study contributes to the existing knowledge of the machining of Ti5553 alloy. Comparative research studies were performed, using various machining environments. Wear mechanisms and chip characteristics were studied. Relationships among cutting speed, coolant pressure, the tool material, wear mechanisms, and tribological aspects of the cutting (cutting forces and chips characteristics) were evaluated. Based on the goals established at the start of this thesis, and considering the experimental procedure developed to achieve those goals, the following conclusions may be drawn, based on the results obtained.

- Machining performance: Considering the four selected cutting tools to develop this study, the tool life of PCD1U is almost 28% longer than that of PCD2U tool. This result is supported not only by SEM figures, but also by the tool wear studies. Additionally, the predominant tool wear mechanism is abrasion. That occurs due to the hardness of titanium and molybdenum presents in the microstructure of Ti5553.

- Oxidation wear is noticeably less intensive when HPC is used, suggesting less severe sliding interactions at the end of the tool-chip contact length.

- The use of HPC facilitates chip control, resulting in better chip evacuation and a significant reduction in chip curl radius. This is due to the additional bending moment added to the chip's undersurface.

- Tool forces: Lower cutting forces when MQL was applied indicate that this coolant mode can improve the friction coefficient in comparison the other coolant methods. When machining low thermal conductivity material, however, high temperatures are found in the cutting region, so this method cannot provide enough cooling to minimise heat build up this application. As a result, oxidation wear is increased over time, and tool life is decreased in comparison with the HPC mode.

- Chip analysis: The PCD1U configured in MQL coolant mode provides the best tribological cutting conditions. As a result, when compared to flood and dry modes, this combination decreases friction and increases tool life.

- Surface integrity: The results show that MQL produces lower compressive stress, while surfaces obtained by machining under Flood and HPC show surface hardening and high residual stress. The application of MQL to the improvement of friction conditions, on the other hand, improved the surface finish and, as a result, decreased the hardening effect on the surface as well as the microstructural damage to the part.

6. Suggestions for future work

Based on the current study, several topics are suggested for further experimental investigations:

- Evaluation of temperature distribution during the cutting process for the mentioned tools and coolants.

- Evaluation of the use of a cryogenic system as a coolant to improve the tool wear performance.

- In order to transfer this technology to the aerospace industry, a study of technical and economical viability is recommended.

References

[1] M. Darecki *et al.*, “Flightpath 2050,” *Flightpath 2050 Eur. Vis. Aviat.*, p. 28, 2011, doi: 10.2777/50266.

[2] S. C. Gad, “Titanium,” in *Encyclopedia of Toxicology*, Elsevier, 2014, pp. 584–585.

[3] N. Clément, “Phase transformations and mechanical properties of the Ti-5553 β-metastable titanium alloy,” p. 314 p., 2010, [Online]. Available: http://hdl.handle.net/2078.1/32266.

[4] E. Tascioglu, A. Gharibi, and Y. Kaynak, “High speed machining of near-beta titanium Ti-5553 alloy under various cooling and lubrication conditions,” *Int. J. Adv. Manuf. Technol.*, vol. 102, no. 9–12, pp. 4257–4271, Jun. 2019, doi: 10.1007/s00170-019-03291-3.

[5] E. O. Ezugwu, R. Batista Da Silva, W. Falco Sales, and A. Rocha Machado, “Overview of the Machining of Titanium Alloys,” in *Encyclopedia of Sustainable Technologies*, vol. 2, Elsevier, 2017, pp. 487–506.

[6] E. M. Trent, *Metal Cutting*, no. 2. London: Butterworths, 1983.

[7] M. C. Shaw, *Metal Cutting Principles*, no. 2. New York: Oxford University Press, 2002.

[8] G. Lütjerin and J. C. Williams, *Titanium*. Berlin, Heidelberg: Springer, 2007.

[9] P. J. Arrazola, A. Garay, L. M. Iriarte, M. Armendia, S. Marya, and F. Le Maître, "Machinability of titanium alloys (Ti6Al4V and Ti555.3)," *J. Mater. Process. Technol.*, vol. 209, no. 5, pp. 2223–2230, 2009, doi: 10.1016/j.jmatprotec.2008.06.020.

[10] Veiga C., Devim J. P., and Loureiro A. J. R., "Properties and applications of titanium alloys: a brief review," *Rev. Adv. Mater. Sci.*, vol. 32, no. 2, pp. 133–148, 2012.

[11] V. Wagner, M. Baili, and G. Dessein, "The relationship between the cutting speed, tool wear, and chip formation during Ti-5553 dry cutting," *Int. J. Adv. Manuf. Technol.*, vol. 76, no. 5–8, pp. 893–912, 2014, doi: 10.1007/s00170-014-6326-1.

[12] Q. Zhao, F. Yang, R. Torrens, and L. Bolzoni, "PM versus IM Ti-5Al-5V-5Mo-3Cr Alloy in Mechanical Properties and Fracture Behaviour," vol. 22, 2019.

[13] Z. Wang- and X. Wang, "Mechanical properties of heat treated Ti-5Al-5V-5Mo-3Cr, an attempt to define critical properties of various microstructural

features.”

[14] M. G. E. P. P.J. Arrazola, Ainhara Garay, Irantzu Sacristán, L.M. Iriarte, Dani Soler, “Mecanizado de aleaciones de titanio empleadas en aeronáutica,” *19 Congr. Máquinas-Herramienta y Tecnol. Fabr. Donostia – San Sebastián*, pp. 1–13, 2013.

[15] F. Products and H. P. R. Drill, “Kennametal,” *Kennametal.com*, 2020. .

[16] E. O. Ezugwu and Z. M. Wang, “Titanium alloys and their machinability—a review,” *J. Mater. Process. Technol.*, vol. 68, no. 3, pp. 262–274, Aug. 1997, doi: 10.1016/S0924-0136(96)00030-1.

[17] C. H. Che-Haron, “Tool life and surface integrity in turning titanium alloy,” *J. Mater. Process. Technol.*, vol. 118, no. 1–3, pp. 231–237, 2001, doi: 10.1016/S0924-0136(01)00926-8.

[18] S. Veeck, D. Lee, R. Boyer, and R. Briggs, “The castability of Ti-5553 alloy: Its microstructure and properties,” *J. Adv. Mater.*, vol. 37, no. 4, pp. 40–45, 2005.

[19] P. Stolf, J. M. Paiva, Y. S. Ahmed, J. L. Endrino, S. Goel, and S. C. Veldhuis, “The role of high-pressure coolant in the wear characteristics of WC-Co tools during the cutting of Ti–6Al–4V,” *Wear*, vol. 440–441, no. October, p.

203090, 2019, doi: 10.1016/j.wear.2019.203090.

[20] R. B. Da Silva, Á. R. MacHado, E. O. Ezugwu, J. Bonney, and W. F. Sales, "Tool life and wear mechanisms in high speed machining of Ti-6Al-4V alloy with PCD tools under various coolant pressures," *J. Mater. Process. Technol.*, vol. 213, no. 8, pp. 1459–1464, 2013, doi: 10.1016/j.jmatprotec.2013.03.008.

[21] M. H. Nouari M, "Experimental investigation on the effect of the material microstructure on tool wear when machining hard titanium alloys: Ti-6Al-4V and Ti-555.," *Int Refract Met Hard Mater*, vol. 41, pp. 259–269, 2013.

[22] S. W. Moura RR, da Silva MB, Machado AR, "The ´ effect of application of cutting fluid with solid lubricant in suspension during cutting of Ti-6Al-4V alloy," in *20th International Conference on Wear of Materials*, 2015, pp. 762–771.

[23] H. Hong, A. T. Riga, J. M. Gahoon, and C. G. Scott, "Machinability of steels and titanium alloys under lubrication," *Wear*, vol. 162–164, no. PART A, pp. 34–39, 1993, doi: 10.1016/0043-1648(93)90481-Z.

[24] H. J. Siekmann, "How to machine Titanium," in *How to machine Titanium*, 1955, pp. 78–82.

[25] Y. Huang, Y. K. Chou, and S. Y. Liang, “CBN tool wear in hard turning: A survey on research progresses,” *Int. J. Adv. Manuf. Technol.*, vol. 35, no. 5–6, pp. 443–453, 2007, doi: 10.1007/s00170-006-0737-6.

[26] Z. C. Lin and D. Y. Chen, “A study of cutting with a CBN tool,” *J. Mater. Process. Tech.*, vol. 49, no. 1–2, pp. 149–164, 1995, doi: 10.1016/0924-0136(94)01321-Q.

[27] A. E. Diniz, F. C. Marcondes, and N. L. Coppini, “Tecnologia da Usinagem dos Materiais,” *Artliber Editora Ltda.* p. 227, 2013.

[28] D. F. XIE Hui, Feng Fei, XU Zhihao, “Study on the characteristics of PCBN materials at home and aboard,” *Diam. Abrasives Eng.*, vol. 38, no. 225, p. 6, 2018, doi: 10.13394/j.cnkijgszz.2018.3.0006.

[29] D. Ferraresi, *Fundamentos da Usinagem dos metais*, 1st ed. São Carlos - Sp: 1971, 1971.

[30] A. K. Syed, J. Hardell, and B. Prakash, “Tribological behaviour of surface-treated and post-oxidized tool steels at room temperature and 400 °C,” *Est. J. Eng.*, vol. 16, no. 2, pp. 123–134, 2010, doi: 10.3176/eng.2010.2.01.

[31] Leonardo Roberto Silva, Odilon Soares Silva, Arthur Hermsdorff Cezar, Santos, and Matheus Barbosa de Medeiros Alvim, “Mecanismos de

Desgaste de Ferramentas no Torneamento Com Alta Velocidade de Corte na Liga Ti-6Al-4V," *An. do IX Congr. Nac. Eng. Mecânica*, no. November, pp. 4–13, 2016, doi: 10.20906/cps/con-2016-0238.

[32] Y. Shokoohi, E. Khosrojerdi, and E. Shekarian, "The effects of concentration of cutting fluids on machining performance during end milling of steel St60," *Mech. Ind.*, vol. 17, no. 4, 2016, doi: 10.1051/meca/2015068.

[33] Y. Shokoohi, "APPLICATION OF SUPERABSORBENT COOLANT AS A NOVEL APPROACH TO SEMI-DRY MACHINING," McMaster, 2018.

[34] W. Liu and Z. Liu, "High-pressure coolant effect on the surface integrity of machining titanium alloy Ti-6Al-4V: a review," *Mater. Res. Express*, vol. 5, no. 3, p. 032001, Mar. 2018, doi: 10.1088/2053-1591/aab44f.

[35] P. Stolf, J. M. Paiva, G. Fox-Rabinovich, and S. C. Veldhuis, "Machinability comparison between two different grades of aerospace alloys under diverse turning conditions: {Ti}-6Al- 4V and {Ti}-5Al-5V-5Mo-3Cr," p. 7, 2018.

[36] F. Klocke, D. Lung, T. Cayli, B. Döbbeler, and H. Sangermann, "Evaluation of Energy Efficiency in Cutting Aerospace Materials with High-Pressure Cooling Lubricant Supply," vol. 15, no. 6, pp. 1179–1185, 2014, doi: 10.1007/s12541-014-0454-2.

[37] Z. Fang and T. Obikawa, “Turning of Inconel 718 using inserts with cooling channels under high pressure jet coolant assistance,” *J. Mater. Process. Technol.*, vol. 247, no. March, pp. 19–28, Sep. 2017, doi: 10.1016/j.jmatprotec.2017.03.032.

[38] K. Weinert, I. Inasaki, J. W. Sutherland, and T. Wakabayashi, “Dry machining and minimum quantity lubrication,” *CIRP Ann. - Manuf. Technol.*, vol. 53, no. 2, pp. 511–537, 2004, doi: 10.1016/S0007-8506(07)60027-4.